

**TECHNICAL UNIVERSITY – GABROVO**  
**Faculty: Mechanical and Precision Engineering**  
**Department: Material Science and Mechanics of Materials**

**Eng. SIMEON TSANKOV TSENKULOVSKI**

**Peculiarities of laser marking of layer-reinforced composites  
on a polymer basis**

**AUTOREFERAT**  
to acquire an educational and scientific degree  
**DOCTOR**

Field of higher education: **5. Technical science**  
Professional field: **5.6. Materials and Material science**  
Scientific specialty: **Material Science and Technology of  
Engineering Materials**

Research supervisor  
**Assoc. Prof., Ph. D, Eng. Ivan Nenov Mitev**

July 2025  
Gabrovo

The dissertation was discussed and sent for official defense at a meeting of the Extended Department Council of the Department of Material Science and Mechanics of Materials at the Faculty of Mechanical and Precision Engineering of the Technical University - Gabrovo, held on 08.07.2025.

The dissertation contains 146 pages and an appendix. The scientific content is presented in an introduction, 5 chapters and a conclusion and includes 74 figures, 22 tables and 1 appendix. 186 literary sources are cited. The numbering of the figures, tables and formulas in the abstract is in accordance with that in the dissertation.

The development of the dissertation was carried out in the Department of Material Science and Mechanics of Materials at the Faculty of Mechanical and Precision Engineering of the Technical University - Gabrovo and in the company "ADTECH" Ltd., Gabrovo

Official presentation of the dissertation will be held on ..... at ..... in Meeting room, Rectorate building of Technical University - Gabrovo.

Author: Eng. Simeon Tsankov Tsenkulovski

e-mail: simeon.tsenkulovski@gmail.com

Title: PECULIARITIES OF LASER MARKING OF LAYER-REINFORCED COMPOSITES ON A POLYMER BASIS

Printing: 3 pcs.

## **GENERAL CHARACTERISTICS OF THE DISSERTATION**

### **Relevance of the problem**

Lasers are a reliable and effective alternative to traditional methods for processing all types of materials. In recent years, the use of lasers for marking materials has increased due to the speed, accuracy and flexibility of this modern technique. At the same time, however, this technology has not been studied sufficiently and the information in the scientific literature on the management and control of these processes is relatively small and incomplete. No scientific aspects can be found regarding the laser marking of products made of various types of composite materials, although in recent years they have found increasingly widespread application in industrial production. In practice, the marking of this type of materials is carried out by applying the "trial-error-correction" principle. The huge variety of composite polymers creates a number of difficulties in the application of laser marking and gives rise to the need to search for a scientific approach to solve them. The thermal, optical and mechanical properties of various polymer-based composites make this area interesting and challenging for optimization and process management. In order to obtain the desired results and quality of the marking, it is necessary to control the process by adjusting the parameters of the laser system to the characteristics of the specific material.

Research of the process of laser marking of layered reinforced polymer matrix composites, which represent a significant part of industrial materials, is an important step towards its clarification in theoretical and experimental aspects. The results obtained will allow for the evaluation and expansion of the practical application of this innovative technology in industry.

### **Purpose and goals of the dissertation work**

The purpose of the dissertation work is to optimize the parameters of the laser marking process of layered reinforced composite materials on a polymer basis.

To achieve the goal set in this study, it is necessary to solve the following tasks:

1. Development of a system for laser marking of layered reinforced composite materials on a polymer basis - formation of a conceptual model and production of a prototype.
2. Selection of materials and research methods.
3. Development of a physical model of the laser marking process of layered reinforced composites on a polymer basis.
4. Study of the influence of technological factors on the quality of marking.
5. Optimization of the technological parameters of the process.

### **Research methods**

The research presented in the dissertation work was carried out using modern and adequate methods and technical means for solving the tasks set. Methods for modeling, statistical processing and analysis of experimental results, planning of experiments and optimization using specialized software were applied.

### **Scientific novelty**

The scientific novelty is concluded in:

- Development of a conceptual model of a laser system for marking layer-reinforced polymer-based composites.
- Construction of graphical dependencies for the influence of the technological parameters of the laser marking process (laser radiation power and marking speed) on the geometric parameters of the laser line (depth, width, and cross-section) formed on samples of textolite and glass textolite.
- Construction of mathematical models for the influence of the studied technological parameters on the depth and width of the marking line in the studied layer-reinforced composite materials.

### **Applicability**

- Based on the developed conceptual model, a system for laser marking has been developed, both on layered reinforced composites and on other non-metallic polymer-based materials.
- The optimal combinations of laser beam power and marking speed have been determined, in order to obtain a marking stroke with appropriate geometric parameters (depth and width).

### **Approbation of the dissertation work**

The dissertation work was reported and discussed at an extended meeting of the Department of Material Science and Mechanics of Materials at the Technical University - Gabrovo.

Stages of the dissertation work were discussed and published in:

- ISPC “Environment Technology Resources”, Rezekne, Latvia, 2023 and 2024
- International Scientific Symposium “Metrology and Metrology Assurance“, 2022 and 2023
- Journal of Industrial Technologies, 2024
- Journal of Technical University of Gabrovo – 2025 r.

### **Structure and volume of the dissertation work**

The dissertation work consists of – table of contents, accepted notations and abbreviations, introduction, 5 chapters, conclusion, classification of contributions, list of publications on the dissertation, used literature and appendix, in a total volume of 146 pages, which contain text, formulas, 74 figures and graphs and 22 tables.

The literature includes 159 titles (articles, reports, books, textbooks, dissertations, reference books and catalogs, standards) and 27 Internet sites. Of the literary sources, 112 are in the Latin alphabet.

## **CONTENTS OF THE DISSERTATION WORK**

### **Chapter One: Laser Marking of Industrial Materials – State of the Problem, Analysis of Existing Solutions**

Laser technologies are found in almost every sphere of life, with one of their most widespread applications being for processing industrial materials by: cutting, welding, marking, engraving, drilling holes, and others - Fig. 1.3.

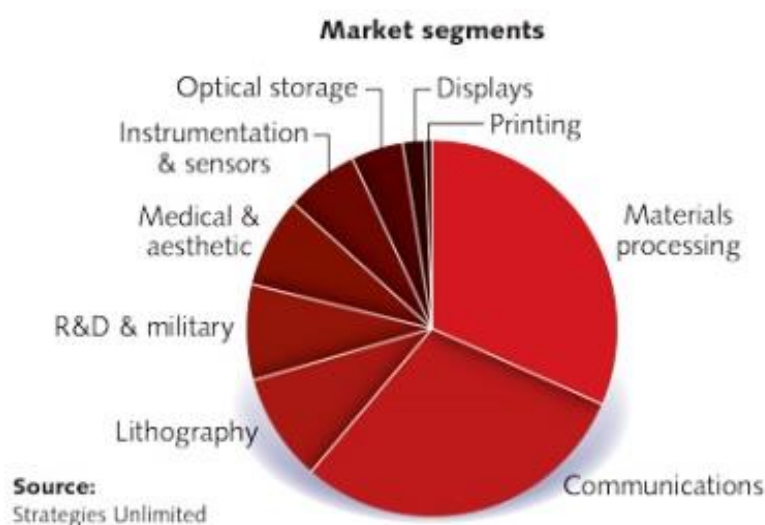


*Fig.1.3. Application of laser technology [123]*

In laser marking of industrial materials, the contrast is of essential importance for the quality of the marking. The factors that influence the contrast can be grouped into four main areas:

- ❑ properties of the marking materials
- ❑ characteristics of the laser source
- ❑ features of the technological process
- ❑ complex properties.

Laser marking systems can be mainly defined as:

- ❑ a process with low operating costs
- ❑ high-speed marking
- ❑ suitable for a wide variety of materials
- ❑ suitable for very fine markings
- ❑ extremely reliable, even in harsh production conditions.

The problems associated with the use of laser marking technology are:

- ❑ Low level of protection. Marking systems are most often of an open type, which creates a constant risk of exposure of operators to laser radiation. The use of personal protective equipment is mandatory, which on the one hand protects the operator, and on the other hand reduces or limits freedom of movement and perception.
- ❑ Low automation. The actions of readjustment and loading of the marking system are performed mainly manually, which in turn leads to a high risk of errors and the creation of rejected production. The accuracy of adjustment and positioning of the parts is subjective and cannot be compensated. The quality of the applied markings is directly dependent on human intervention, which leads to increased requirements for the qualification of the personnel. This also leads to delayed marking processes and work with the part/product, respectively, loss of valuable production time and reduced system productivity.
- ❑ Low communication capabilities. Difficult collection of electronic data on the operations performed on the processed parts. There is no centralized system (server) for registering and processing data from marking. There is no possibility for remote control over the generation of the marking work program and the implementation of process traceability. Inability to make flexible changes to the program during the production processes.

From the available data on laser marking of industrial materials, it can be concluded that in-depth and scientifically based research on this process is insufficient in the scientific literature. There is no data on the physical nature of the process of laser marking of layered reinforced composite materials with a polymer matrix. The interrelation and degree of influence of the various parameters of the technological process (optical and thermophysical properties of the material, etc.) on the quality of the marking has not been clarified. This requires for each specific case to experimentally establish the optimal working intervals to achieve the highest quality at maximum productivity. The lack of systematized information on the laser marking of layered reinforced composite materials on a polymer basis limits the application of this method in industry. For reliable prediction and optimization of the technological process of laser marking of these materials, it is necessary to scientifically study it.

## **Chapter Two: Equipment, Materials and Research Methods**

### ***2.1. Research Equipment***

#### ***2.1.1. Development of a Conceptual Model***

After analyzing the existing solutions for laser marking systems and formulating new possible improvements, the following characteristics of the system are defined:

- ❑ source of laser radiation - Fiber laser
- ❑ laser radiation output power – 50 W
- ❑ protected structure with protective covers and protective glass for monitoring the

- process
- ❑ option to include central aspiration
- ❑ introduction of additional axes of movement:
  - ✓ *planar movement of the laser beam realized by a scanning device*
  - ✓ *linear axes for introducing and removing parts into the marking zone*
  - ✓ *for focusing the laser beam*
  - ✓ *for performing rotation of a part in synchronization with the feed movement in the working area*
- ❑ introduction of servo control of the axes to increase positioning accuracy and improve process repeatability.

The comparative analysis of the conceptual model of a system for laser marking of layered reinforced composites with a polymer matrix with alternative solutions was carried out according to selected indicators. These are dynamic generation of the marking program, servo control of the axes of movement, number of additional axes of movement, need for additional cooling, minimum size of the laser spot, equipment durability, need for consumables and equipment maintenance, optical guidance of the laser radiation with minimal losses, low power consumption for the process, quality and durability of the applied marking.

### 2.1.2. Advantages of the model

With the thus proposed conceptual model for developing a product innovation - a system for laser marking of non-metallic materials, a significant improvement is presented to the laser marking systems currently existing on the market, including:

- ❑ Fiber laser with an average output power of 50 W
- ❑ scanning head XY with a working field of 140x140 mm  
the ability to perform auxiliary movements along three axes:  
linear along the X and Z axes, rotary axis A
- ❑ servo control and motors for driving the axes
- ❑ server for remote control and implementation of dynamic generation of marking programs.

### 2.1.3. Development of a laser system for making layered reinforced composite materials with a polymer matrix

Based on the conceptual model, a laser system for marking with a periphery was developed according to Fig. 2.2. It is based on Fiber laser – RFL- P - 502B with an optical F-theta lens–SL – 1064-150-2106 - Fig. 2.3. The laser marking generator consists of six main nodes - Fig. 2.4.

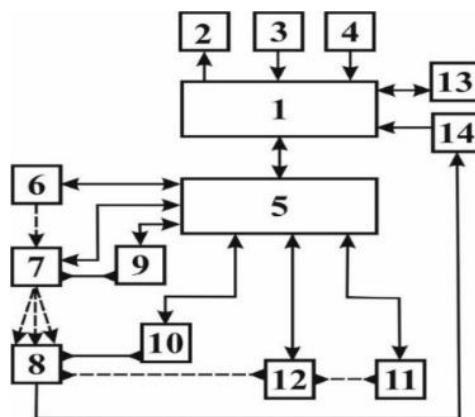


Fig.2.2. Schema of the experimental setup:

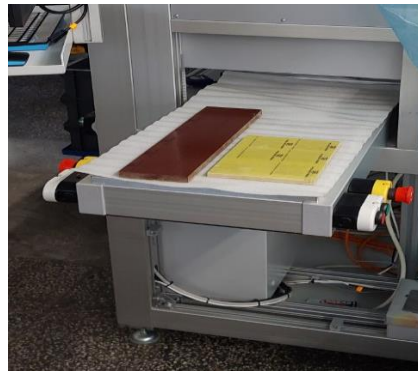
1 – computer; 2 – monitor; 3 – keyboard; 4 – mouse; 5 – controller  
6 – laser radiation source; 7 – scanning device; 8 – sample; 9, 10, 11, 12 – devices for movement along X, Y, Z and rotation around the vertical axis; 13 – server; 14 – barcode reader.



*Fig.2.3. General view of the laser marking system for layered reinforced composites with a polymer matrix*



*a.*



*b.*



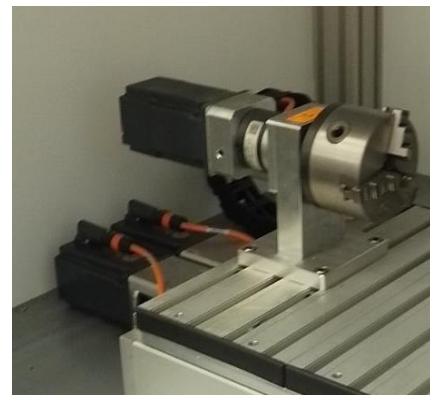
*c.*



*d.*



*e.*



*f.*

*Fig.2.4. Main modules of the marking system:  
a – control panel housing; b – horizontal module; c – vertical module; d – scanning head;  
e – rotating head; f – control cabinet*

## 2.2. Materials for research

For research, layered composite materials on a polymer basis with the reinforcing phase of cotton and glass layers, and the matrix is formed of phenol-formaldehyde and epoxy resins, were selected.

The textolite is 10 mm and mechanical characteristics according to DIN 7753/ PFCC 202, and IEC 60893 Hgw 2082.

The glass textolite is 10mm thick and mechanical characteristics type PTGC 201, according to IEC/EN 60893-3-1.

## 2.3. Research Methods

In the research process, methods were used to determine the geometric parameters of the marking stroke, to measure the average and maximum roughness, and to optimize technological objects.



Fig. 2.7. General view of a PHILIPS URD measuring microscope

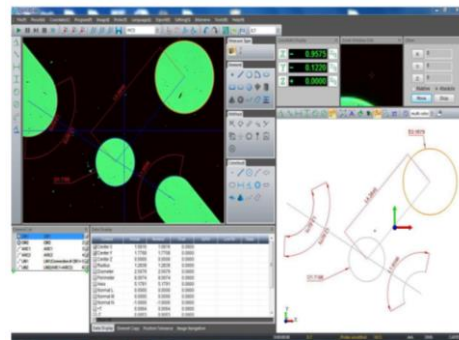


Fig.2.8. Software for 2D and 3D INSIZE ISD – V150



Fig. 2.12. General view of a profilometer ZEISS

The qualitative analysis of the studied samples was performed on a measuring microscope PHILIPS URD – Fig. 2.7. using INSIZE ISD – V150 software – Fig.2.8, and the roughness measurements were made with a portable ZEISS profilometer - Fig. 2.12, which is compatible with the following standards: DIN 4762, DIN 4768, DIN 4771, DIN 4775 DIN 4766-1.

## Chapter Three: Elements of the Energy Balance in Laser Marking of Layered Polymer Composites

### 3.1. Interaction of the Laser Beam with the Substance in Local Processing of Non-Metallic Materials

Local laser processing of the material is the result of the appearance and use of powerful light fluxes that act on the surface of the processed product. It can be considered as the localization of the thermal effect to the maximum extend along the radius –  $r$ , of the beam (most often along the Gaussian distribution of the surface power density) and in the depth of the material – along the  $z$  axis – Fig.3.1.

Depending on the transparency of the material at  $\delta \ll d_f$  a surface heat source is formed with a different distribution of the absorbed power density -  $W(r, z)$  - Fig.3.2.



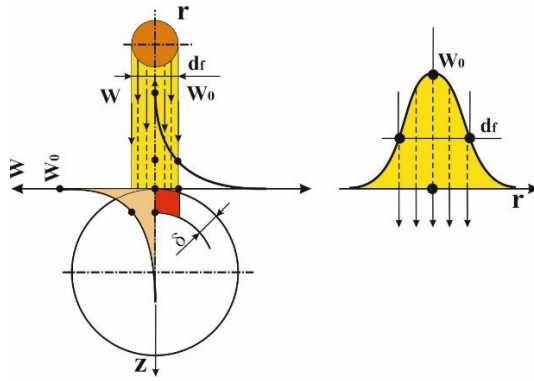


Fig.3.1. schematic diagram of the local surface laser thermal impact on non-metallic materials depending on the penetration depth –  $\delta$  and the size of the sample -  $r$

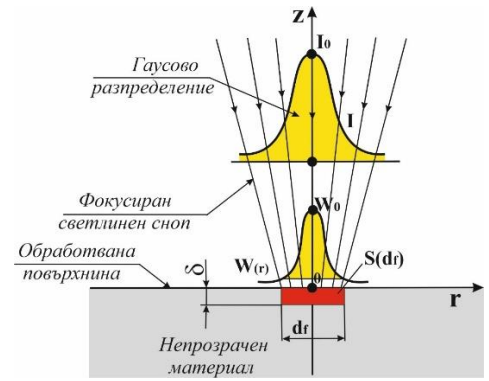


Fig.3.2. Formation of a surface secondary heat source in an opaque material

In the processing of non-metallic materials, the normal Gaussian distribution is the most common law for defining the power density –  $I(r)$ , in the normal cross section of the energy beam (or in the contact spot). The corresponding local heat source is also characterized by a normal distribution of the surface density of the absorbed power –  $W(r)$ , and can be calculated by 3.1:

$$W_{(r)} = W_0 \cdot e^{-k \cdot r^2} = A \cdot I_0 \cdot e^{-k \cdot r^2} \quad (3.1)$$

where:  $k$  – flow concentration coefficient characterizing the shape of the normal distribution curve.

The heat power of the local heat source (3.2) can be obtained by integrating the surface power density  $W(r)$  over the surface of the contact spot -  $S_f = \pi \cdot r_f^2$ .

$$P_0 = \int_{(s)} W_{(r)} \cdot dF = \left(\frac{\pi}{k}\right) \cdot W_0 \cdot (1 - e^{-k \cdot r_f^2}) \quad (3.2)$$

Depending on the way the energy of the incident light beam is absorbed, we can distinguish two typical cases:

- continuous absorption during the penetration of the light beam into the material
- penetration of the light beam into the material to a certain depth -  $\delta_z$ , without absorption, after which the absorption is distributed evenly in all directions with continuous attenuation with distance from the center (diffusive scattering).

When processing non-metallic materials with radiant heat exchange during laser processing, there is continuous absorption of energy in the depth of the material.

Therefore, we can determine the penetration depth by 3.5:

$$\delta = \frac{1}{\alpha} \quad (3.5)$$

where:  $\alpha$  – absorption coefficient of the light wave.

The dependence of absorption on the penetration depth (Bouguer-Lambart law) is valid for a uniform distribution of the power density –  $W_0$ , in the energy spot of interaction with diameter  $d_f$  – Fig.3.4.

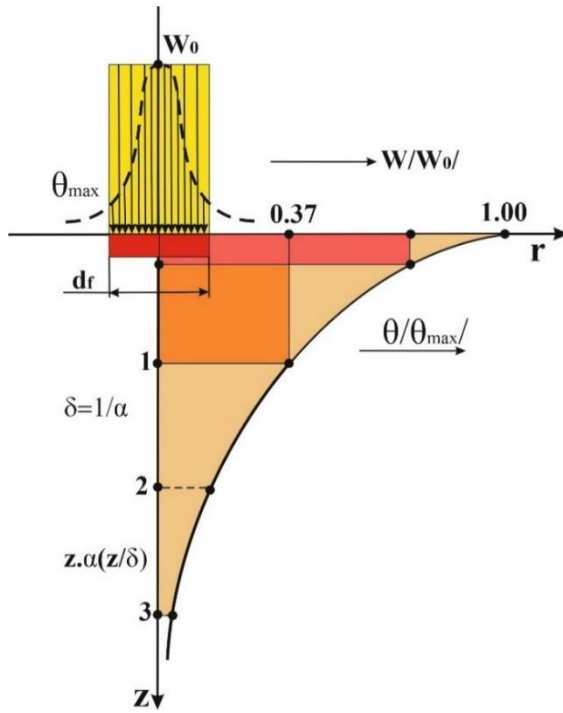


Fig.3.4. Surface energy distribution (relative power density  $W/W_0$  and relative overheating  $\Theta/\Theta_{max}$ ) during laser processing

$$\frac{W}{W_0} = e^{\alpha \cdot z} \text{ или } \frac{W}{W_0} = e^{-\delta \cdot z} \quad (3.6)$$

$$\text{where: } \delta^2 = \frac{\rho}{\pi \cdot \mu \cdot f}$$

Therefore, in beam processing of non-metallic materials and a Gaussian distribution of the surface density of the absorbed power in the contact spot, the depth distribution of the processed area can be determined by 3.7:

$$\frac{W}{W_0} = e^{\left\{ - \left[ \left( \frac{2r}{d_f} \right)^2 + \frac{z}{\delta} \right] \right\}} \quad (3.7)$$

From what has been found, it follows that as a result of laser marking polymer layered composites, structural and/or chemical processes occur, leading to markings with different characteristics.

When the laser beam is directed at the processed material, its energy is transformed into heat, which changes the physical and mechanical characteristics of the material through evaporation, combustion (carbonization), melting or other structural transformations.

The laser acts with high power densities of  $10^8 \div 10^{11} \text{ W.m}^{-2}$  and pulse durations between  $10 \text{ ns} \div 10 \text{ } \mu\text{s}$ , on a certain area of the material, as a result of the focusing of the beam, the heating is very intense in a small area (a few tenths of a micrometer). A very important parameter is the penetration depth –  $\delta$  (3.5) in the substance, as almost all the energy of the laser beam is absorbed and heats it. The penetration depth depends on the optical and thermophysical properties of the material. A distance of  $\delta = 10 \text{ nm}$  the light beam in polymer matrixes passes in the time of  $1 \text{ ns}$ .

This absorbed energy is converted into heat in time of  $t < 10^{-9} \text{ s}$ , being quickly transferred to the material, which in turn becomes a heat source. The heat is distributed differently depending on the type of material. This leads to structural and phase transformations, melting and/or evaporation. Part of the molten liquid (melt) is thrown out of the irradiation zone under the influence of the surface pressure caused by the intense evaporation of the material. The remaining part is heated for a very short time and begins to boil, where it is released in the form of gas, i.e. a phase transformation from liquid to gaseous state occurs again.

### 3.2. Stages of the laser marking process of non-metallic

For composite materials with a polymer matrix, the thermal effect of the laser radiation is expressed in increasing the temperature at which four processes occur, which cause changes in their chemical and/or physical properties – table 3.1.

Depending on the type of material and the temperature reached, laser marking is carried out by one or more of the processes discussed above: structural changes, depigmentation, color change, burning (carbonization) melting and evaporation.

The processes occurring during laser marking of the main non-metallic industrial materials are presented in Table 3.2.

Table 3.1. Stages of the laser marking process

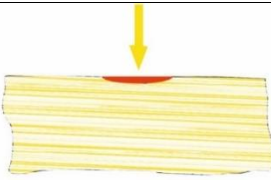
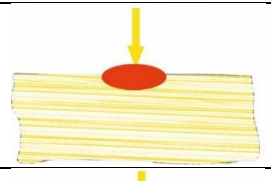
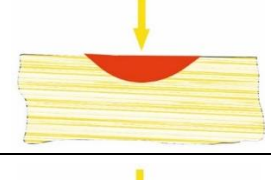
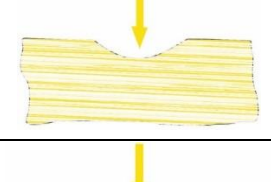

Process	Schema	Phase	Mechanism
<b>Softening</b> – heating below melting temperature $T^o$		Change in structure, color, darkening bleaching.	Destruction of the polymer chain, photo-degradation, oxidation.
<b>Foam-like structure</b>		Formation of gas bubbles	Partial degradation of the material
<b>Melting</b> – heating above melting point $T^o$		Structural and color changes	Recrystallization into glass
<b>Evaporation</b> – heating above the $T^o$ of evaporation or destruction		Forming channels without changing the color, scribing	Conversion from liquid or solid to gaseous state and carbonization
		Forming channels with a color different from the base material	Removing layers deposition on the base material, ablation

Table 3.2. laser marking processes for non-metallic materials

Process	Material			
	Polymer	Glass	Ceramic	Silicon
Ablation	O-	O+	O-	O+
Fragmentation		O+		
Oxidation	O-			
Melting	O-	O+	O-	O+
Destruction	C++	C+	C+	
Foam	C++			
Bleaching	C+			
Color change	C++	C++		
Carbonization	C++			
Dehydration	C++			
<b>Notes:</b> O → change in reflectance, C → change in color - low contrast, + normal contrast, ++ very good contrast				

### 3.3. Elements of the energy balance

The processes occurring in the material depend mainly on the power density ( $q_s$ ) and the exposure time of the laser radiation ( $t_{vd}$ ), as well as on the optical and thermophysical characteristics of the processed material. The intensity of the incident radiation decreases with depth after passing through a layer of substance of a certain thickness.

One part of the luminous flux –  $E$ , of the laser beam incident on the processed material is reflected from its surface –  $E_R$ , another is absorbed –  $E_A$ , and a third passes through it –  $E_D$ . if this dependence is expressed in terms of energy, it will have the form 3.8:

$$E = E_R + E_A + E_D \quad (3.8)$$

where:  $E$  – energy of the incident radiation  
 $E_A$  – energy of absorbed radiation  
 $E_R$  – energy of reflected radiation  
 $E_D$  – energy of transmitted radiation.

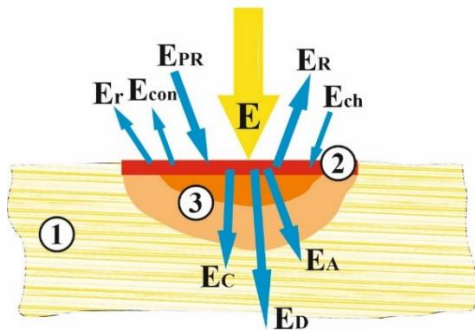


Fig. 3.6. Energy balance diagram for marking layered reinforced polymer matrix composites

During the interaction of the laser beam with the material of the sample 1 - Fig.3.6, additional energy is also obtained in the processing zone 2 as a result of the occurrence of other possible processes, such as: chemical reactions -  $E_{ch}$  – oxidation,  $E_c$  – energy passed into the heat-affected zone 3 around the working area,  $E_r$  – energy of radiation emission,  $E_{con}$  – energy loss from convection,  $E_{PR}$  – energy of the technological process – energy for heating, melting, and/or evaporation.

Therefore, when marking the materials we studied, the energy of the laser beam ( $E$ ), that falls on the samples is transformed into different energies and the energy balance equation can be written – 3.9:

$$E = E_A + E_R + E_D + E_{PR} + E_{ch} + E_c + E_r + E_{con} \quad (3.9)$$

Since the heating of the material occurs at a very high speed (in a very short time), followed by rapid cooling, the energy losses from convection -  $E_{con}$  and radiation -  $E_r$ , are negligibly small. As a result of the thermal conductivity of the material, the heat also spreads through the depth of the part, but the heat affected zone is small because the time is short and the values of -  $E_c$ , are small. As a result of the reflection from the surface, energy losses occur ( $E_R$ ), and part of the energy is lost from its passage through the material ( $E_D$ ). Taking into account the losses for the energy required for marking, we can write equation 3.10:

$$E_A + E_{ch} = E_{PR} + E_c \quad (3.10)$$

### 3.4. Conclusions

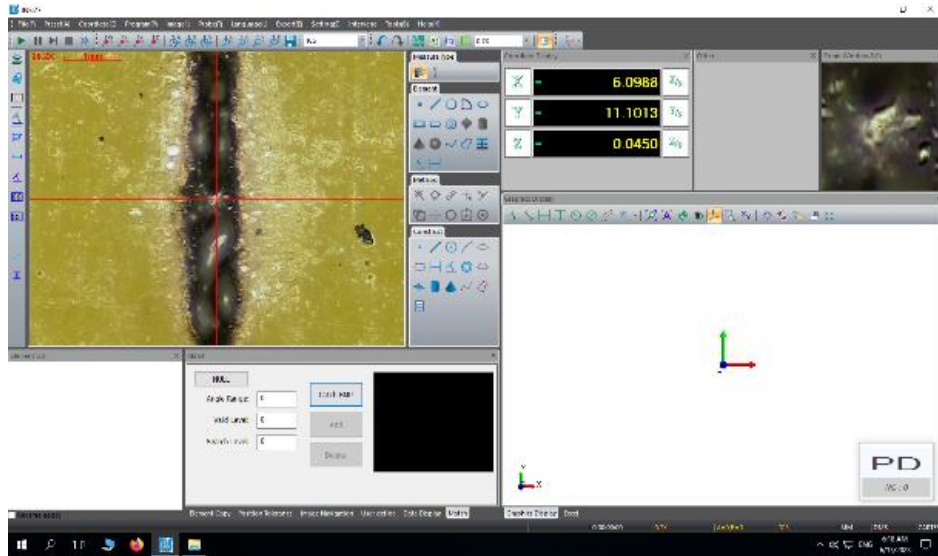
1. Local heat sources in laser processing of non-metallic opaque materials are characterized by a temperature distribution field that follows the distribution of the absorbed energy density -  $W(r,z)$
2. When processing non-metallic materials with a laser-type heat source, the maximum temperature is registered on the surface of the material.
3. Four stages have been identified in the process of laser marking on non-metallic materials – softening, formation of a foam-like structure, melting and evaporation.

## Chapter Four: Determining the Technological Parameters of the Process

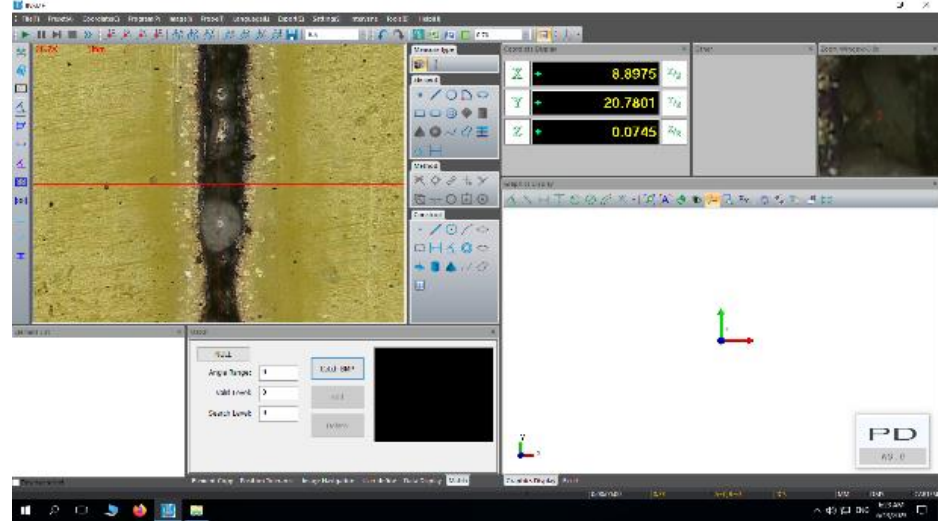
### 4.1. Influence of technological parameters on the depth of marking

The main technological parameters in laser marking speed and the output of the laser installation. To determine their influence on the depth of the marked strokes, experiments were made on marking with a speed  $V = 50 \div 250$  mm/s, output power  $P = 5 \div 50$  W, pulse frequency  $f = 50$  kHz and focal spot diameter 40  $\mu$ m.

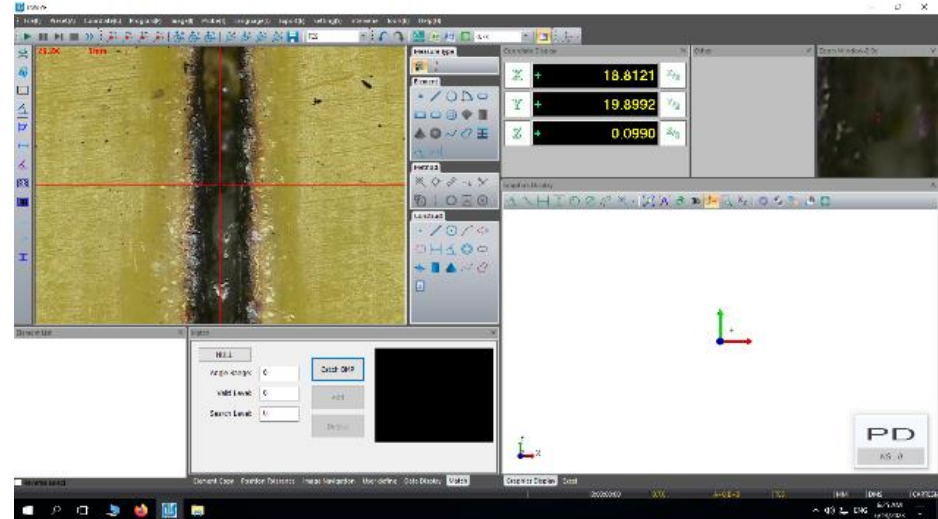
Measurements of the penetration depth –  $\delta$   $\mu$ m, were determined at 5 control points located along the marked line at a distance of 10 mm. Part of the measurements are presented in Fig. 4.3 and 4.4, and all experimental results are presented in Tables 4.1 and 4.2 respectively for glass textolite and textolite samples, and their graphic interpretation in Fig. 4.9 and 4.10.



a.



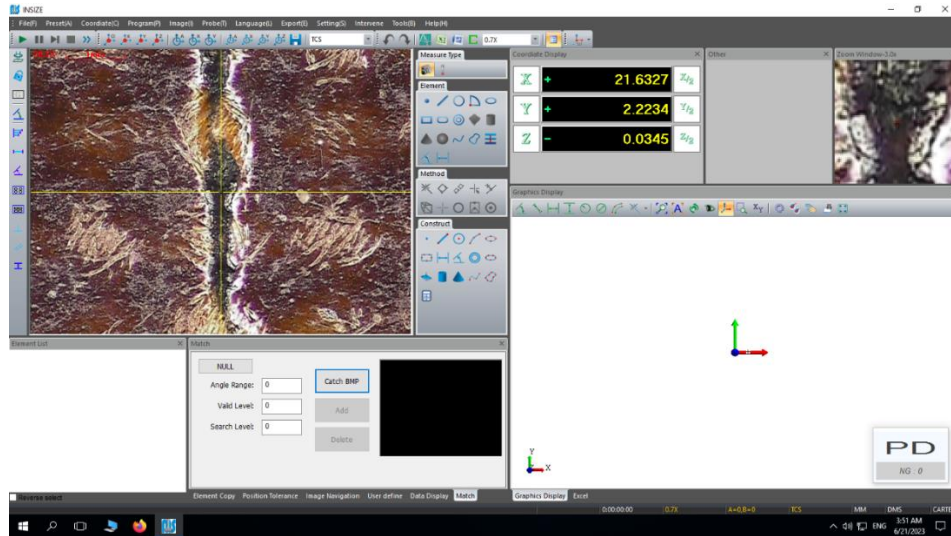
b.



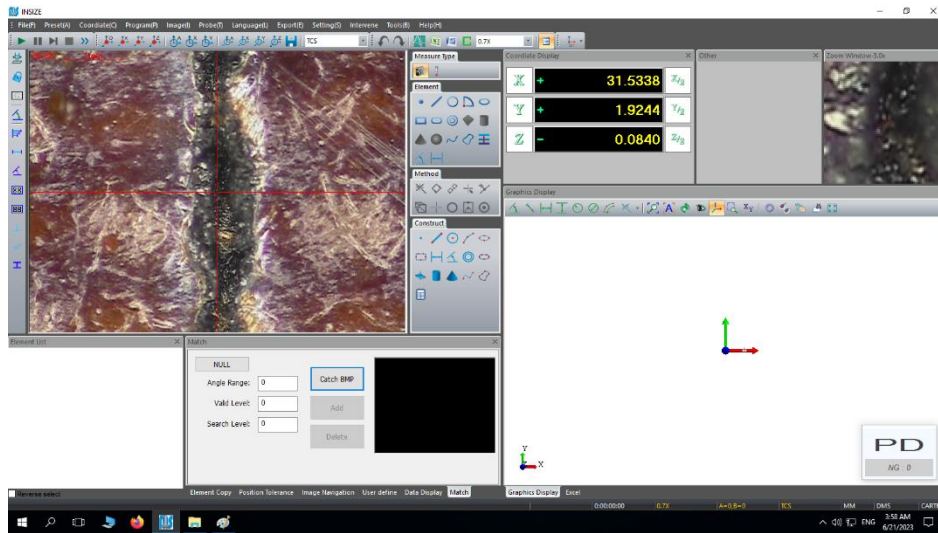
c.

Fig.4.3. Experimental results on marking glass textolite with  $V=50$  mm/s and  $f= 50$  kHz,  $\times 10$   
a – 25 W; b – 40 W; c – 50 W.

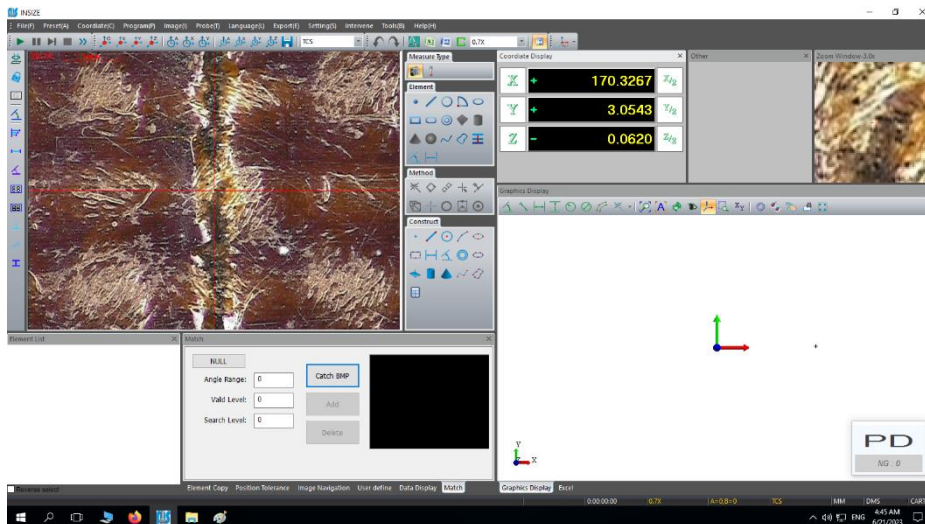




a.



b.



c.

Fig.4.4. Experimental results on marking textolite with  $V=50$  mm/s and  $f=50$  kHz,  $\times 10$   
a – 25 W; b – 35 W; c – 50 W.

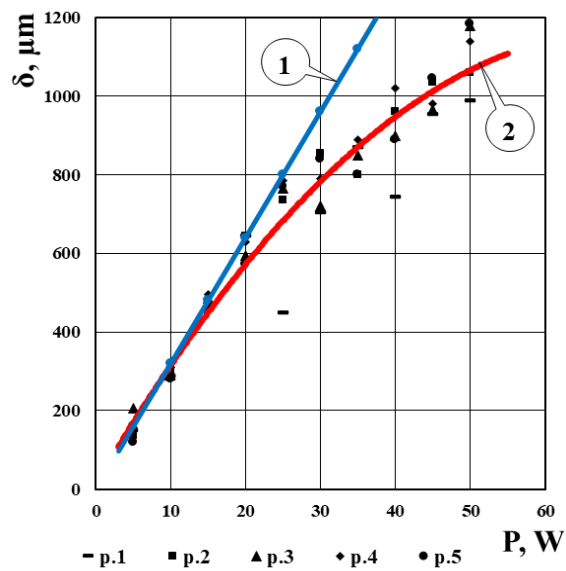
Table 4.1 Experimental results for glass textolite samples

No	P, W	$\delta, \mu\text{m}$						
		p.1	p.2	p.3	p.4	p.5	$\Sigma p_1 \div p_5 / 5$	$\delta_{\text{max}}, \mu\text{m}$
1	2	3	4	5	6	7	8	9
<b>V= 50 mm/s</b>								
1	5	150	135	205	155	120	153	160
2	10	280	305	300	310	280	295	320
3	15	456	466	485	495	454	471	480
4	20	645	645	595	630	573	618	640
5	25	450	735	765	785	770	701	800
6	30	705	855	720	790	840	782	960
7	35	870	800	850	890	800	842	1120
8	40	745	960	900	1020	890	903	1280
9	45	955	1035	965	980	1045	996	1440
10	50	990	1060	1180	1140	1185	1111	1600
<b>V= 100 mm/s</b>								
11	5	65	76	75	70	64	70	78
12	10	155	148	149	156	132	148	156
13	15	225	230	232	214	234	227	234
14	20	274	280	308	305	278	289	312
15	25	307	320	305	308	285	305	391
16	30	410	388	400	395	407	400	469
17	35	442	420	393	388	417	412	547
18	40	506	531	525	504	534	520	625
19	45	625	600	598	586	591	600	703
20	50	515	500	522	485	503	505	781
<b>V= 150 mm/s</b>								
21	5	49	50	50	51	52	51	52
22	10	105	100	98	97	103	101	104
23	15	145	138	140	150	137	142	156
24	20	174	192	185	179	180	182	208
25	25	217	189	205	194	200	201	260
26	30	255	252	250	247	276	256	312
27	35	365	345	360	355	365	358	365
28	40	410	416	415	414	415	414	417
29	45	392	345	354	374	370	367	469
30	50	401	347	355	341	346	358	521
<b>V= 200 mm/s</b>								
31	5	35	34	37	38	35	36	39
32	10	76	78	70	75	78	75	78
33	15	110	115	110	110	116	112	117
34	20	150	145	152	155	155	151	156
35	25	185	185	185	190	185	186	195
36	30	223	231	220	225	226	225	234
37	35	255	245	258	251	256	253	274
38	40	310	312	305	310	313	310	313
39	45	275	279	301	270	260	277	352
40	50	302	314	322	306	286	306	391
<b>V= 250 mm/s</b>								
41	5	25	31	30	31	29	29	31
42	10	55	60	60	64	55	58	63
43	15	90	93	89	86	91	90	94
44	20	125	115	120	120	111	118	125
45	25	155	151	147	145	151	150	156
46	30	180	175	178	171	175	176	188
47	35	213	207	205	201	213	208	219
48	40	240	251	235	239	234	240	250
49	45	270	265	255	275	275	268	281
50	50	310	305	298	295	305	303	313

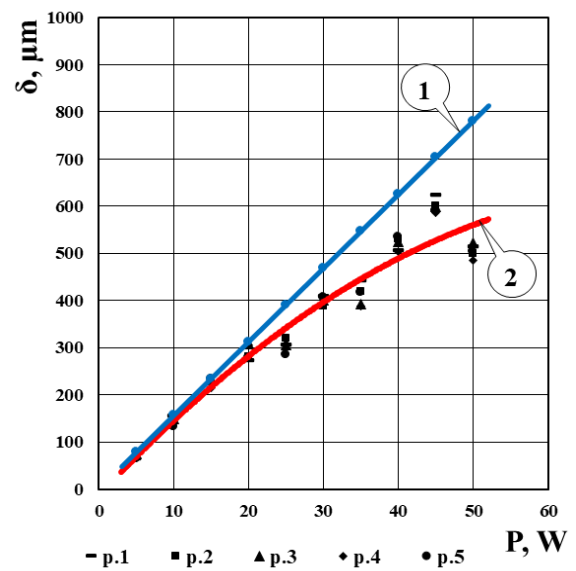
Table 4.2 Experimental results for textolite samples

No	P, W	$\delta, \mu\text{m}$						
		p.1	p.2	p.3	p.4	p.5	$\Sigma p_1 \div p_5 / 5$	$\delta_{\text{max}}, \mu\text{m}$
1	2	3	4	5	6	7	8	9
<b>V= 50 mm/s</b>								
1	5	85	94	85	90	90	89	91
2	10	162	164	161	150	158	159	182
3	15	220	232	225	224	219	224	273
4	20	315	298	290	288	269	292	364
5	25	405	398	397	402	413	403	455
6	30	476	492	490	480	497	487	546
7	35	610	605	608	618	599	608	636
8	40	725	720	710	709	721	717	727
9	45	701	700	708	705	706	704	818
10	50	667	655	658	660	685	665	909
<b>V= 100 mm/s</b>								
11	5	45	40	42	40	43	42	45
12	10	85	85	90	88	92	88	91
13	15	125	110	114	121	100	114	136
14	20	142	145	155	146	122	142	182
15	25	199	201	190	195	205	198	227
16	30	245	251	250	255	234	247	273
17	35	308	292	295	300	310	301	318
18	40	364	355	363	362	356	360	364
19	45	332	329	317	332	320	326	409
20	50	341	350	338	337	334	340	455
<b>V= 150 mm/s</b>								
21	5	25	30	35	25	35	30	30
22	10	54	59	65	65	57	60	61
23	15	90	85	90	90	95	90	91
24	20	115	115	120	125	117	118	121
25	25	130	127	135	130	138	132	152
26	30	165	160	161	168	161	163	182
27	35	205	210	212	210	203	208	212
28	40	240	242	240	240	238	240	242
29	45	215	210	214	216	205	212	273
30	50	225	231	224	230	220	226	303
<b>V= 200 mm/s</b>								
31	5	25	12	14	25	26	21	23
32	10	42	45	46	45	48	45	46
33	15	65	67	75	70	63	68	68
34	20	95	81	95	85	95	90	91
35	25	115	110	115	98	99	107	114
36	30	135	125	131	135	138	132	136
37	35	150	155	150	153	158	153	159
38	40	180	165	180	175	175	175	182
39	45	195	205	185	195	190	194	205
40	50	205	190	185	184	181	189	227
<b>V= 250 mm/s</b>								
41	5	0	10	0	41	27	16	18
42	10	26	19	40	44	35	33	36
43	15	55	35	60	50	55	51	55
44	20	75	75	75	70	65	72	73
45	25	75	95	75	75	100	86	91
46	30	106	102	95	107	95	101	109
47	35	125	110	115	125	115	118	127
48	40	145	145	125	125	120	132	146
49	45	140	160	155	125	135	143	164
50	50	180	175	170	180	170	175	182

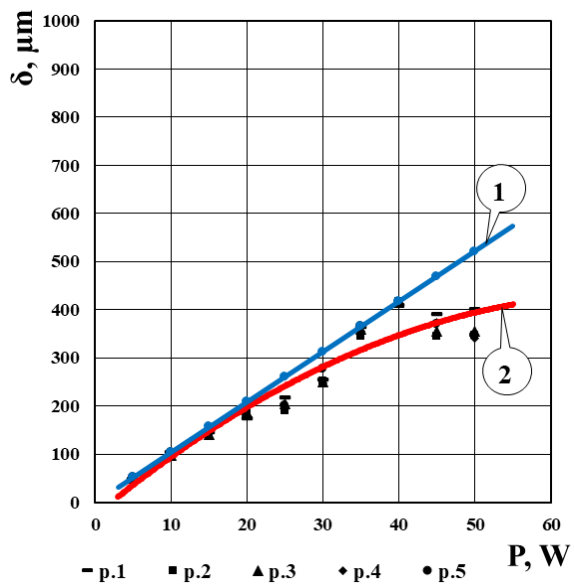




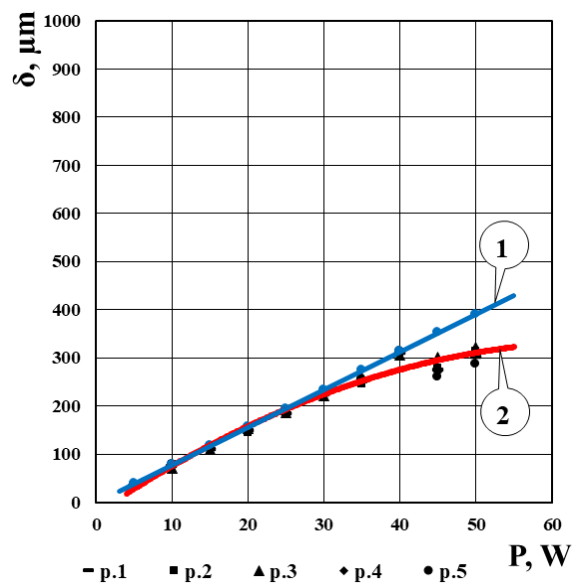
a.



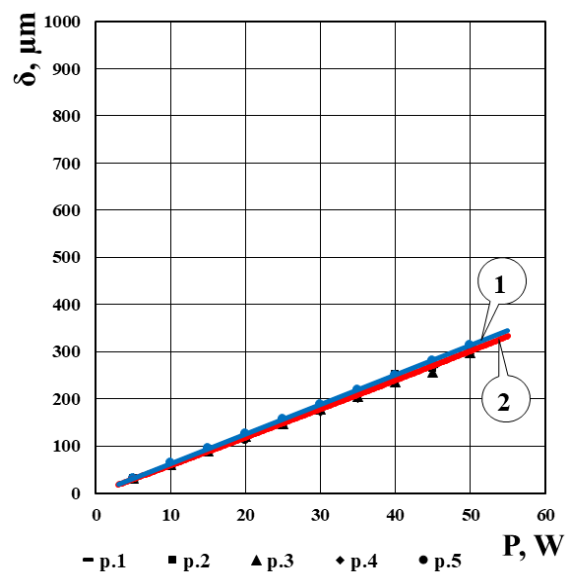
b.



c.



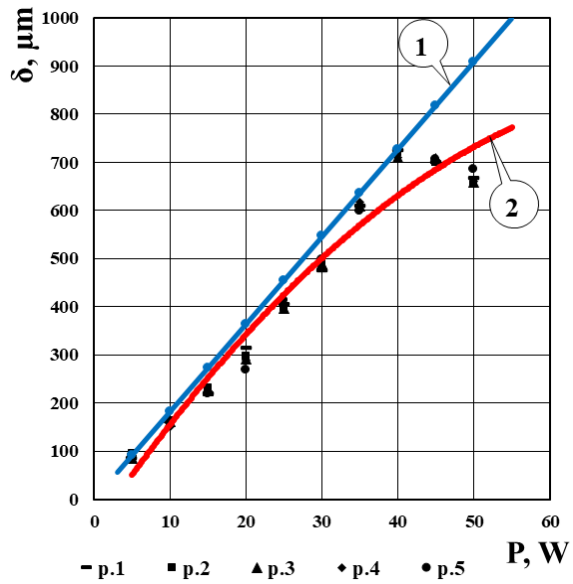
d.



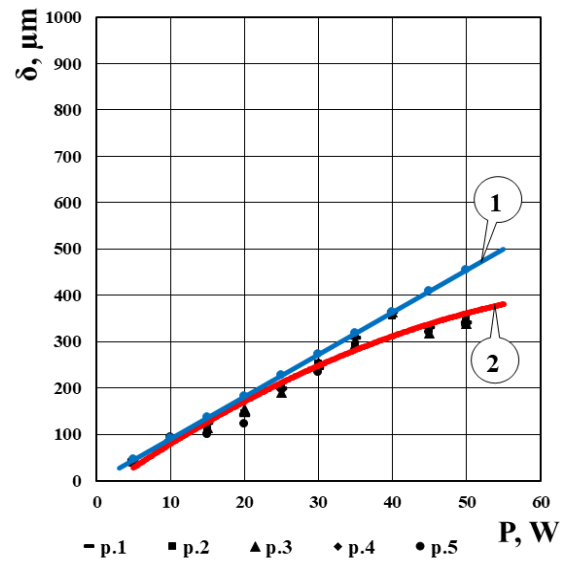
e.

Fig.4.9. Change in depth of laser marking on glass textolite samples depending on the power of the laser radiation at a frequency of 50 Hz and speed:

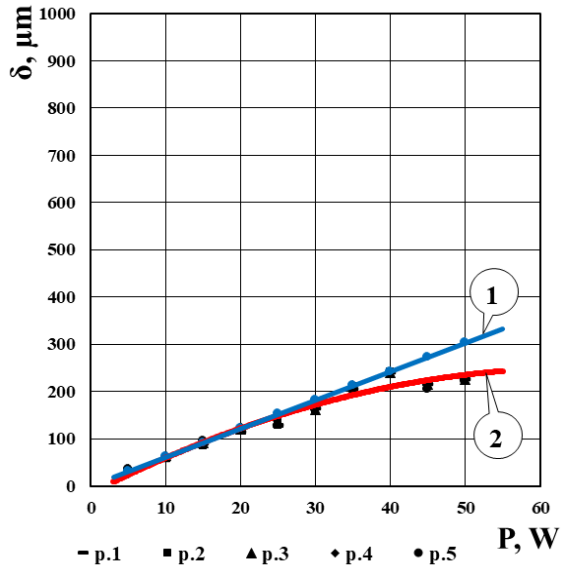
- 1 –  $\delta_{\text{max}}$  (theoretical)
- 2 –  $\delta_{\text{cp}}$  (experimental)
- a – 50 mm/s; b – 100 mm/s;
- c – 150 mm/s; d – 200 mm/s;
- e – 250 mm/s.



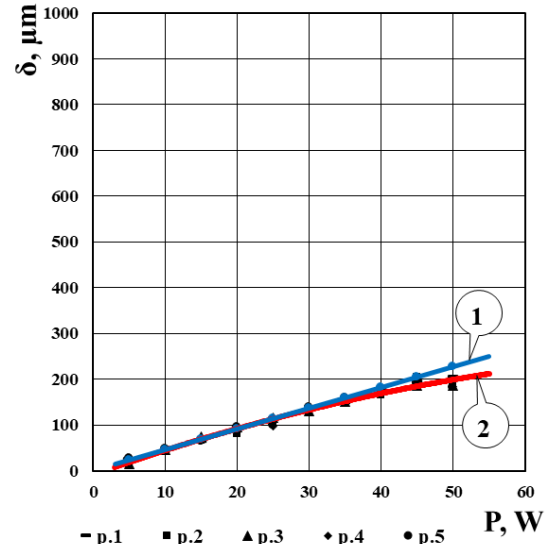
a.



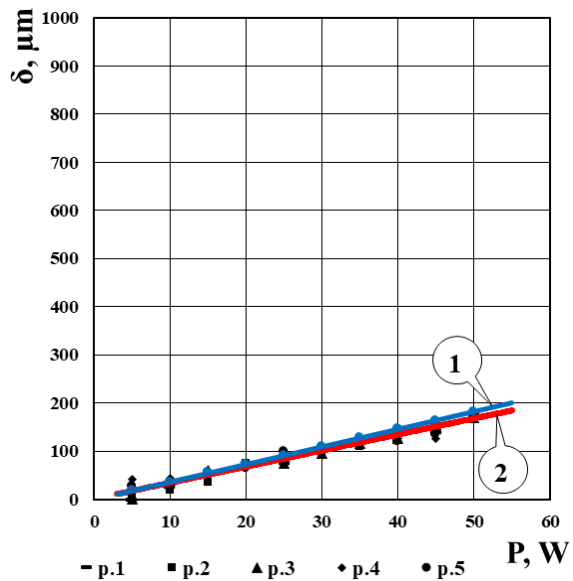
b.



c.



d.



e.

Fig.4.10. Change in depth of laser marking on textolite samples depending on the power of the laser radiation at a frequency of 50 Hz and speed:

- 1 –  $\delta$  max (theoretical)
- 2 –  $\delta_{cp}$  (experimental)
- a – 50 mm/s; b – 100 mm/s;
- c – 150 mm/s; d – 200 mm/s;
- e – 250 mm/s.

Theoretically, non-metallic materials, the maximum penetration depth of the laser beam –  $\delta_{max}$ , can be calculated using expression 4.1 [19]:

$$\delta_{max} = \frac{2P}{\pi \cdot r \cdot \rho \cdot v \cdot c \cdot T} \quad (4.1)$$

where: P – laser radiation power, W  
r – focal spot radius,  $\mu\text{m}$   
 $\rho$  – material density,  $\text{g/cm}^3$   
v – marking speed, mm/s  
c – specific heat of the material, cal/g. $^{\circ}\text{C}$   
T – evaporation temperature,  $^{\circ}\text{C}$ .

Using reference data, the maximum theoretical values of the penetration depth during laser marking of the studied materials have been calculated (column 9 of Tables 4.1 and 4.2). According to 4.1, the penetration depth is linearly dependent on the power of the laser radiation. The experimental results obtained when marking the samples show that this is valid only at low marking powers – up to 20W. In these cases, the experimental results differ from the theoretical ones by less than 10% (Table 4.3).

With increasing output power values above 20 W, the difference in the measured values from the marking depth for glass textolite samples increases from 4 to 30%. The largest differences are recorded for samples marked at a minimum speed – 50÷100 mm/s. at high marking speeds, the differences decrease, and at a speed of 250 mm/s, the experimental results practically overlap with the theoretically calculated ones.

The results for marking textolite samples are similar.

At output power up to 15W, the obtained results differ by 10÷15%, with an increase in output power above 15W, the differences in the measured values range from 4 to 27%. At high marking speeds – 200÷250 mm/s, the difference between the measured and theoretical curves are minimal - below 10% and in practice they overlap.

With increasing marking speed from 50 to 250mm/s, the depth of the marking strokes decreases by about 5÷7 times for both materials studied by us, which is a result of the shorter time for thermal impact on the studied surfaces.

In all studied marking modes, the results for glass textolite samples are better than those obtained on textolite samples. This is explained by the reflectivity of the material – R. it is defined by the ratio 4.2.

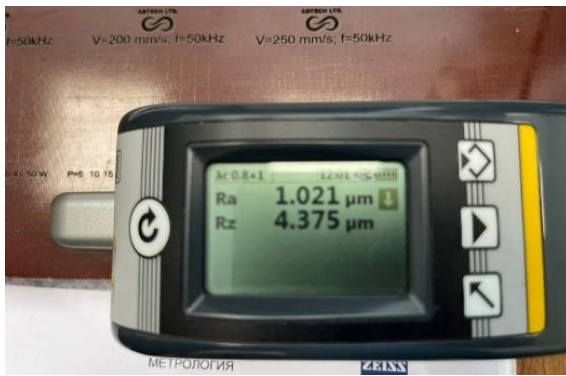
$$R = \frac{J_T}{J_0} \quad (4.2)$$

where:  $J_T$  – intensity of the reflected beam  
 $J_0$  – intensity of the incident radiation.

The reflectivity – R, mainly depends on the condition of the threatened surface. Its main characteristic is the roughness class. As the roughness class of the threatened surface increases, its reflectivity decreases. Roughnesses of the order of the wavelength significantly increase the penetration depth of the laser beam.

In this case, the wavelength is  $\lambda=1.06 \mu\text{m}$ .

The measured roughness of the marked samples is shown in Fig.4.11.



a.



b.

Fig. 4.11. Surface roughness values of:  
a – textolite samples; b – glass textolite samples

It can be seen that the textolite samples the average roughness –  $R_a$ , is close to the length of the laser radiation, but the values for  $R_z$  are over 4 times greater than the wavelength. This leads to significant scattering of the radiation power and reduced values of  $\delta$ .

For the glass textolite samples Fig. 4.11b, the values of  $R_a$  are  $0.225 \mu\text{m}$  and are over 4 times smaller than the wavelength, and for  $R_z = 1.703 \mu\text{m}$  they are commensurate with the length of the incident wave. This also explains the differences in the values of  $\delta$ , for the two studied materials.

Based on the experimental results obtained from Tables 4.1 and 4.2, graphical dependences for the influence of the marking speed on the depth of the formed marking strokes are presented, which are shown in Fig. 4.12. and 4.13. respectively for samples of textolite and glass textolite.

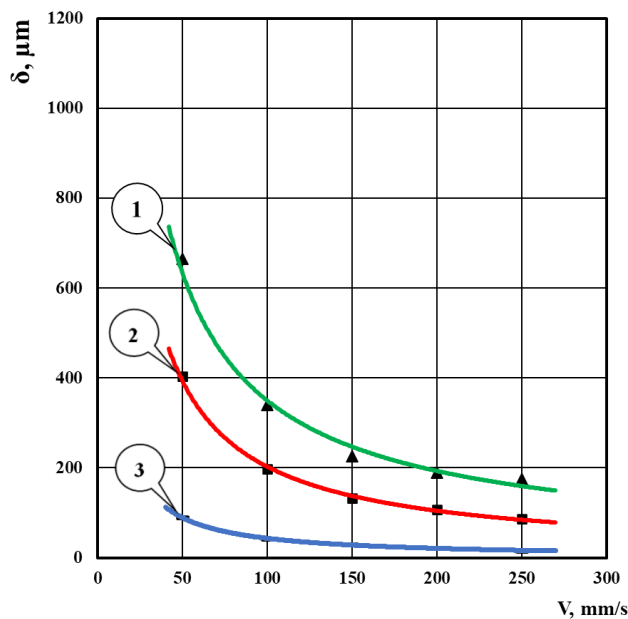


Fig.4.12. Influence of marking speed on the depth of marking on textolite samples at output power:  
1 – 50 W; 2 – 25 W; 3 – 5 W

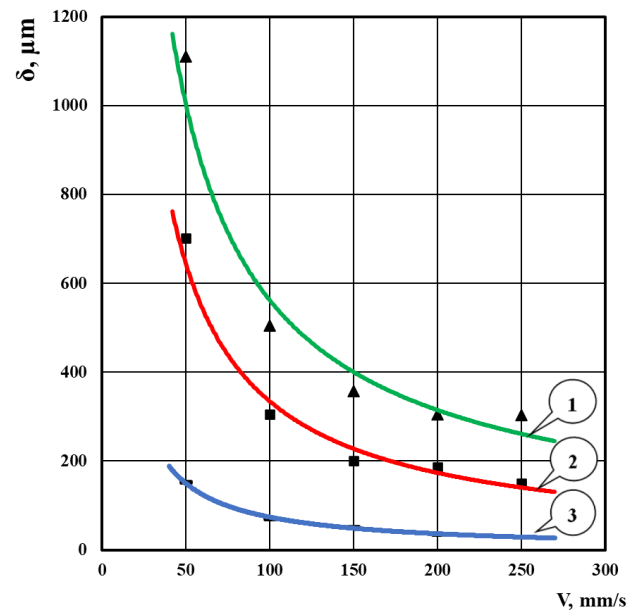


Fig.4.13. Influence of marking speed on the depth of marking on the glass textolite at output power:  
1 – 50W; 2 – 25W; 3 – 5W

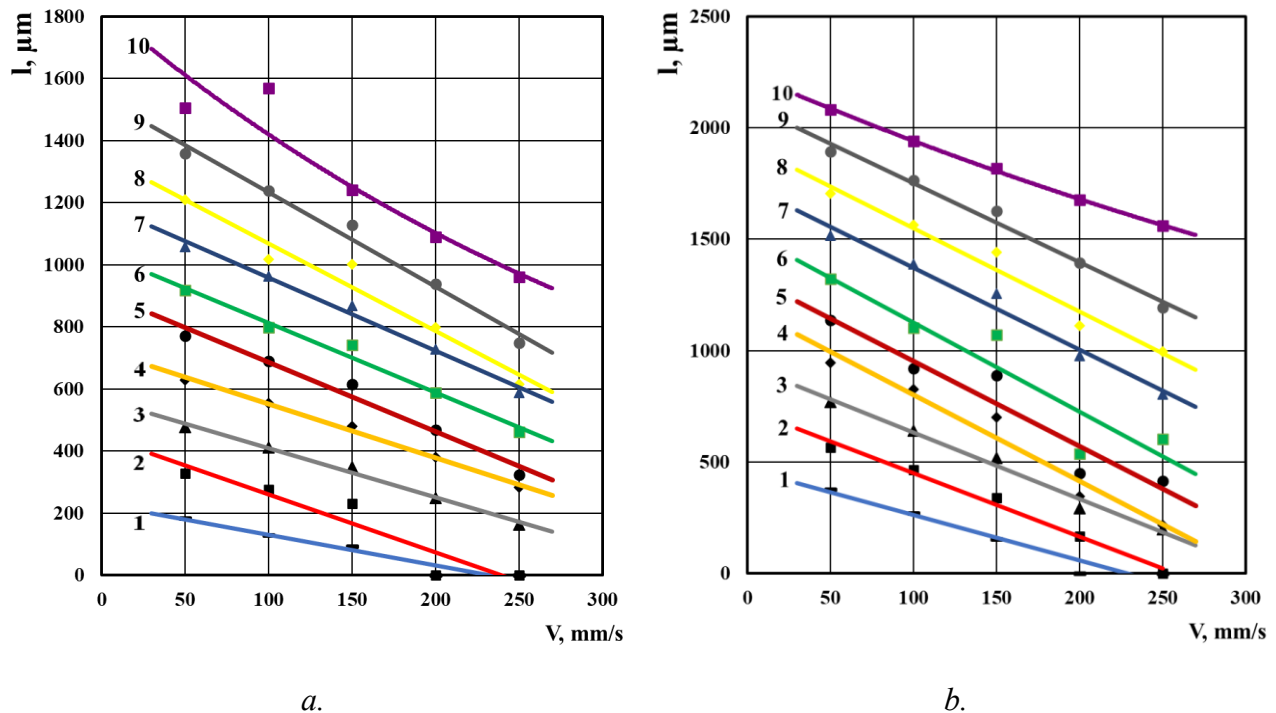
#### 4.2. Influence of technological parameters on the width of the marking

With similar characteristics of the technological parameters of the laser marking process from point 4.1, changes in the width of the marking stroke –  $l$ ,  $\mu\text{m}$ . The graphical interpretation of the

results for the influence of the marking speed and the power of the laser radiation on the width of the marking stroke is shown in Fig. 4.14. and 4.15.

The figures show that the dependencies of the width of the marking stroke on the power of the laser radiation and the marking speed are linear.

The maximum width when marking textolite samples is achieved at maximum power – 50 W and a minimum beam speed of 50mm/s - 1500 $\mu$ m. At a beam power of 50W, with an increase in the marking speed from 50 to 250mm/s, the marking width decreases from 1500 to 960  $\mu$ m –  $\approx$  1.6 times.



*Фиг.4.14. Influence of marking speed on stroke width at different values of output power for samples of: a – textolite; b – glass textolite:*

*1 – 5 W; 2 – 10 W; 3 – 15 W; 4 – 20 W; 5 – 25 W; 6 – 30 W; 7 – 35 W;  
8 – 40 W; 9 – 45 W; 10 – 50 W*

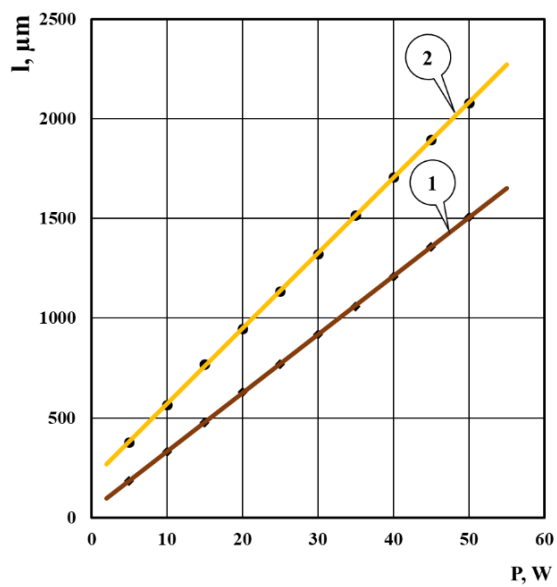
For glass textolite samples, the results obtained are similar. The maximum marking width is achieved at a power of 50 W and a speed of 50 mm/s – 2080  $\mu$ m. At a radiation power of 50 W, with an increase in the marking speed from 50 to 250 mm/s, the marking width decreases.

At a constant marking speed 50 mm/s and an increase in the laser beam power from 5 to 50W, the marking width from textolite samples increases from 180 to 1500  $\mu$ m –  $\approx$  8 times, and for glass textolite samples from 177 to 2080  $\mu$ m –  $\approx$  12 times.

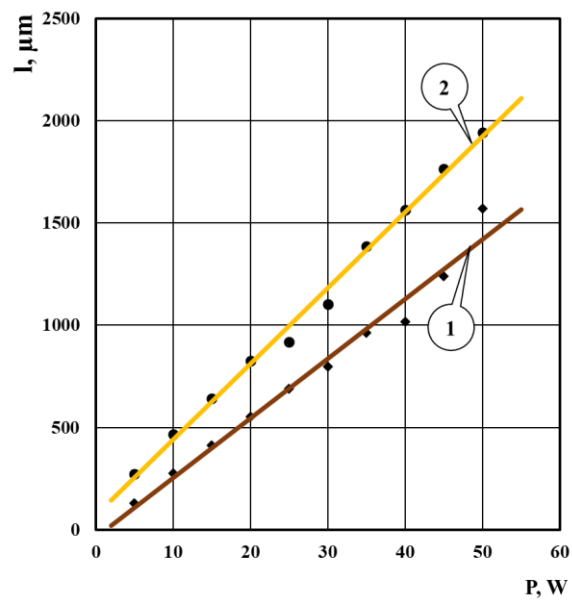
Comparing the experimental results obtained from the two types of samples studied, it is seen – Fig.4.15, that the marking width for glass textolite samples is larger in all the studied marking modes compared to that on textolite samples. The most significant difference is at high radiation powers, where the marking values for glass textolite are 1.25÷1.55 times higher compared to those obtained on textolite samples from 2080 to 1560  $\mu$ m –  $\approx$  1.3 times.

The larger width of the marking on glass textolite samples, similar to the results in point 4.1, can be explained by the smaller roughness on the marked surface compared to that of textolite samples. It should be added that the values of Martens heat resistance and specific heat of textolite samples (Table 2.1) are 160  $^{\circ}$ C and 0.446 cal/g. $^{\circ}$ C, respectively, and are significantly higher compared to those of glass textolite (Table 2.2) 105  $^{\circ}$ C and 0.20 cal/g. $^{\circ}$ C, respectively.

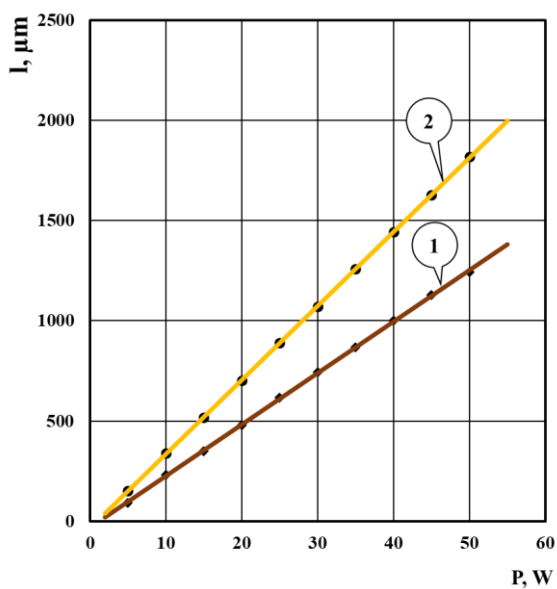
This predetermines the need for a smaller amount of heat to melt the matrix phase of glass textolite samples compared to those made of textolite and the presence of unmarked areas of marking at powers up to 10W and high marking speeds - 150÷250 mm/s.



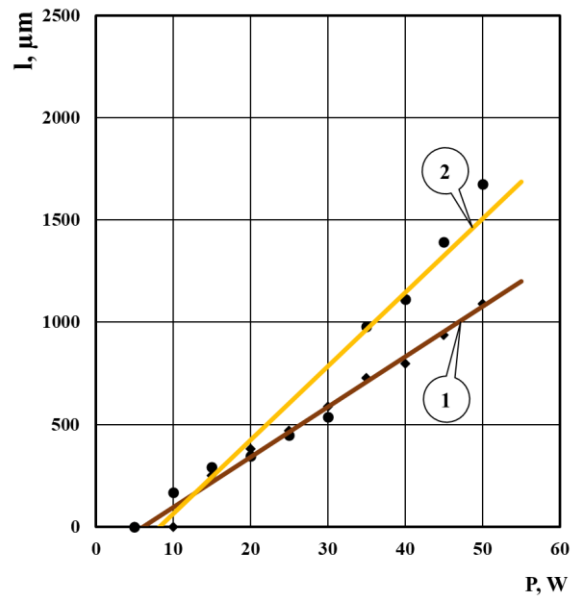
a.



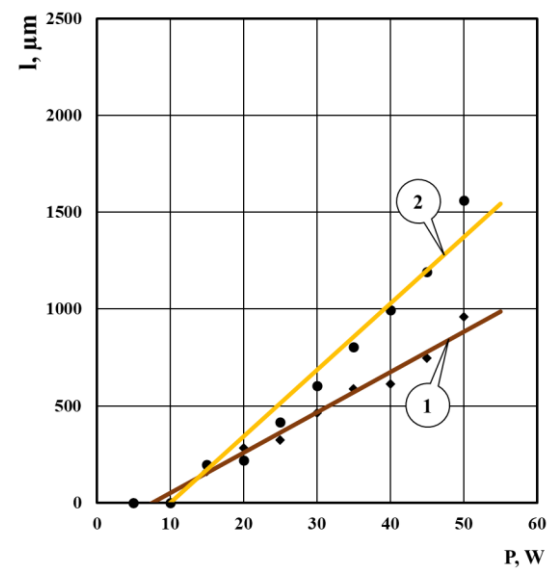
b.



c.



d.



e.

Fig.4.15. influence of output power of the marking for samples of:

1 – textolite;

2 – glass textolite.

a –  $V=50 \text{ mm/s}$ ; b -  $V=100 \text{ mm/s}$ ;

c -  $V=150 \text{ mm/s}$ ; d -  $V=200 \text{ mm/s}$ ;

e -  $V=250 \text{ mm/s}$ ;

### 4.3. Influence of technological parameters on the profile of the cross-section of the marking stroke

When analyzing the results from the literature sources [94, 95, 100, 102, 105] it was found that during laser marking of metal industrial materials the presence of three types of marking channels is observed. They are described in the most detailed way in the studies of the nickel-cobalt alloy “Inconel 718” [100]:

- ❑ Markings in which all points of the profile are positive, and the marking stroke is completely or partially closed – Fig. 4.16 a
- ❑ Markings in which the point of the profile resemble a Gaussian distribution (raised upper edge –  $Z \geq 0$  and negative lower edge –  $Z \leq 0$ ) – Fig. 4.16 b
- ❑ Markings where the profiles are quasi-flat, as in Fig. 4.16c and when the magnification is changed the points of the profile resemble a Gaussian profile.

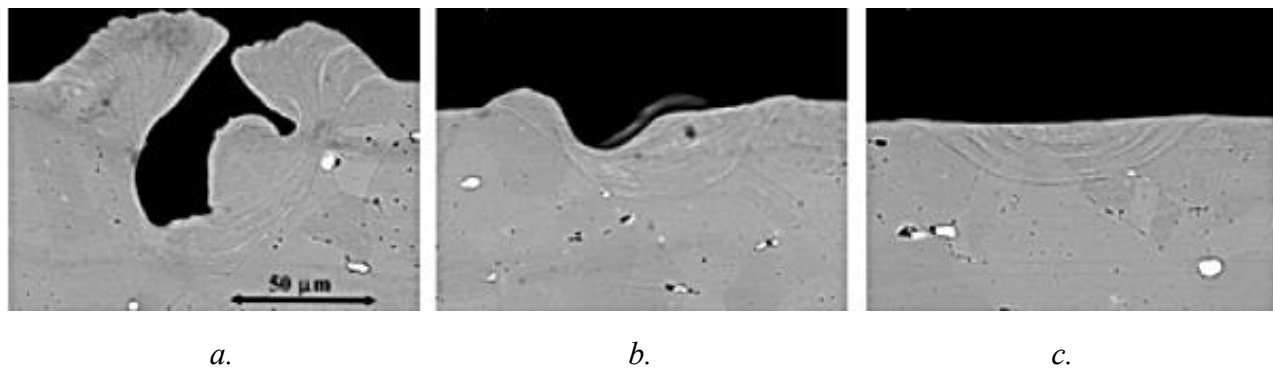


Fig.4.16. Profile of cross-sections of markings obtained on samples of “Inconel 718” [100]

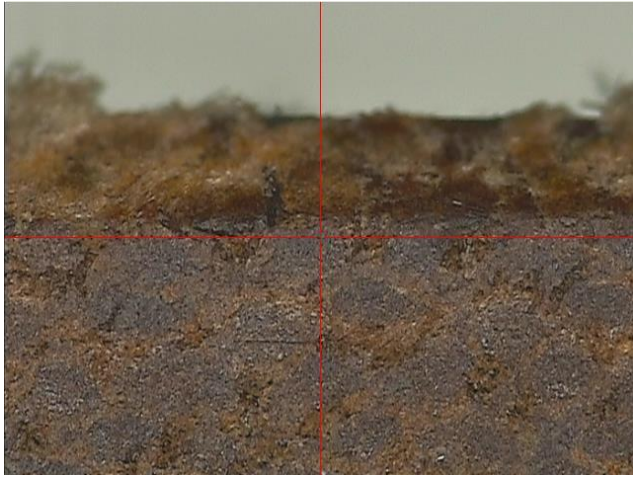
To determine the influence of technological parameters on the profile of the cross-sectional area of the marking in composite layer-reinforced materials with a polymer matrix, the influence of the radiation power –  $P$ , W and the frequency of the laser pulses –  $f$ , kHz.

From the experimental results obtained in points 4.1 and 4.2, it was found that optimal geometric parameters of the marking line are obtained at a marking speed  $V_c = 50$  mm/s and a laser pulse frequency  $f = 50$  kHz. In this regard, experiments to study the profile of the cross-sectional area of the marking channel were carried out at these technological parameters. The experimental results obtained at different power values are presented in Fig.4.17 and 4.18 for samples of textolite and glass textolite, respectively, and for the influence of the frequency of the laser pulse on the channel profile in Fig. 4.19 and 4.20.

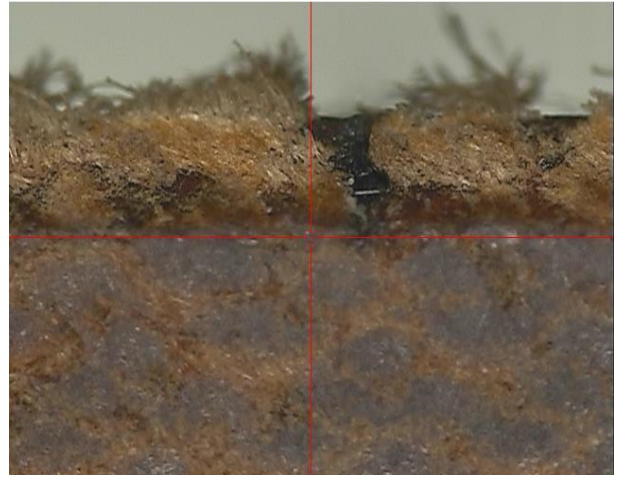
From Fig.4.17 and 4.18 it is seen that with increasing laser radiation power from 10 to 50 W the marking profile changes from pseudo-planar to one resembling a Gaussian distribution of points on the contour. This is more pronounced in the textolite samples – Fig.4.17, because the textolite reinforcing phase has a lower thermal resistance compared to the glass one.

The results of the influence of the laser pulse frequency on the transverse profile of the channel show that with increasing frequency from 50 to 80 kHz, the profile of the marking channel changes from a Gaussian distribution of the contour to pseudo-planar. This is a result of the weaker thermal impact of the radiation in the depth of the processed material at a constant beam speed and constant power.

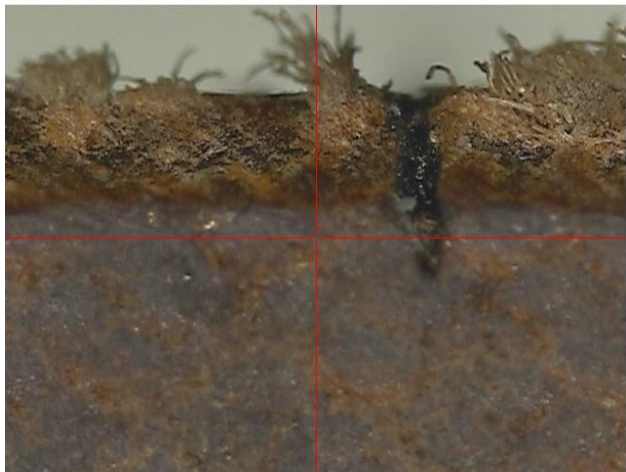




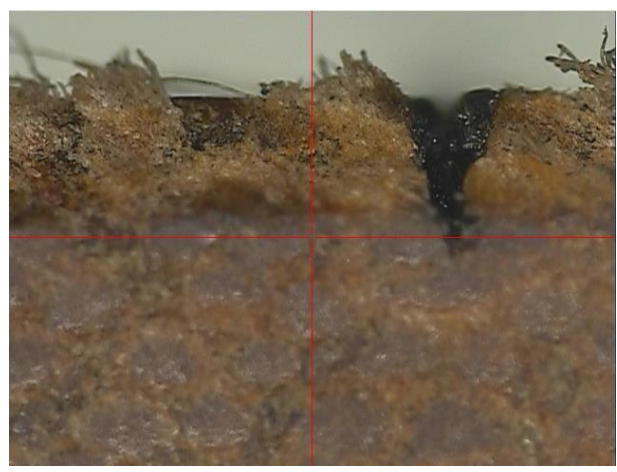
*a.*



*b.*



*c.*



*d.*



*e.*

*Fig.4.17. Influence of the laser radiation power on the profile of the marking stroke when marking textolite samples with the marking mode:  $V_c = 50 \text{ mm/s}$  and  $f = 50 \text{ kHz}$ ,  $\times 30$*

*a –  $P = 10 \text{ W}$ ; b –  $P = 20 \text{ W}$ ;*

*c –  $P = 30 \text{ W}$ ; d –  $P = 40 \text{ W}$ ;*

*e –  $P = 50 \text{ W}$ ;*

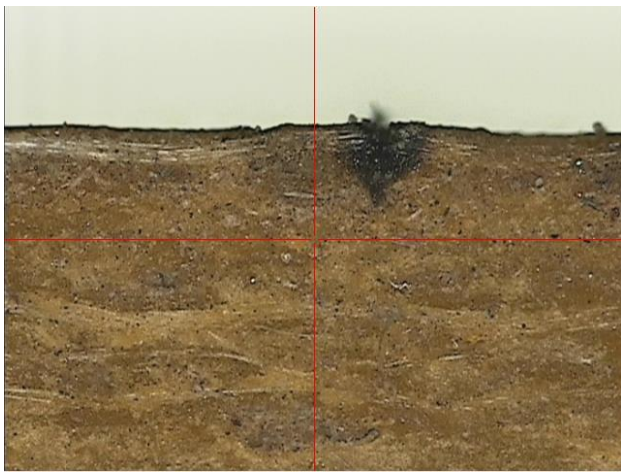




*a.*



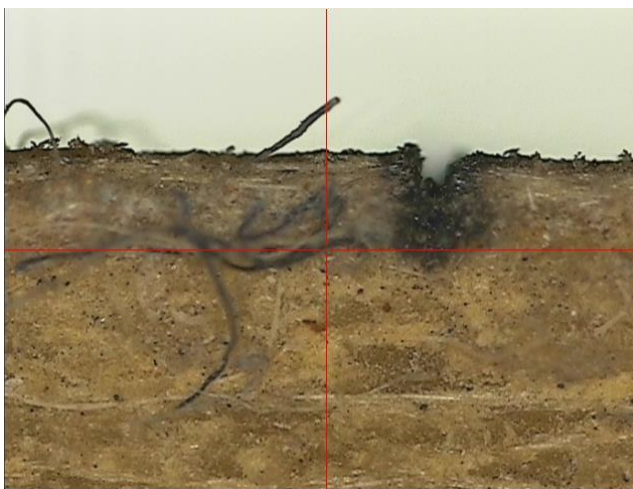
*b.*



*c.*



*d.*



*e.*

*Fig.4.18. Influence of the laser radiation power on the profile of the marking stroke when marking glass textolite samples with the making mode:*

*$V_c = 50 \text{ mm/s}$  and  $f = 50 \text{ kHz}$ ,  $\times 15$*

*$a - P = 10 \text{ W}$ ;  $b - P = 20 \text{ W}$ ;*

*$c - P = 30 \text{ W}$ ;  $d - P = 40 \text{ W}$ ;*

*$e - P = 50 \text{ W}$ ;*

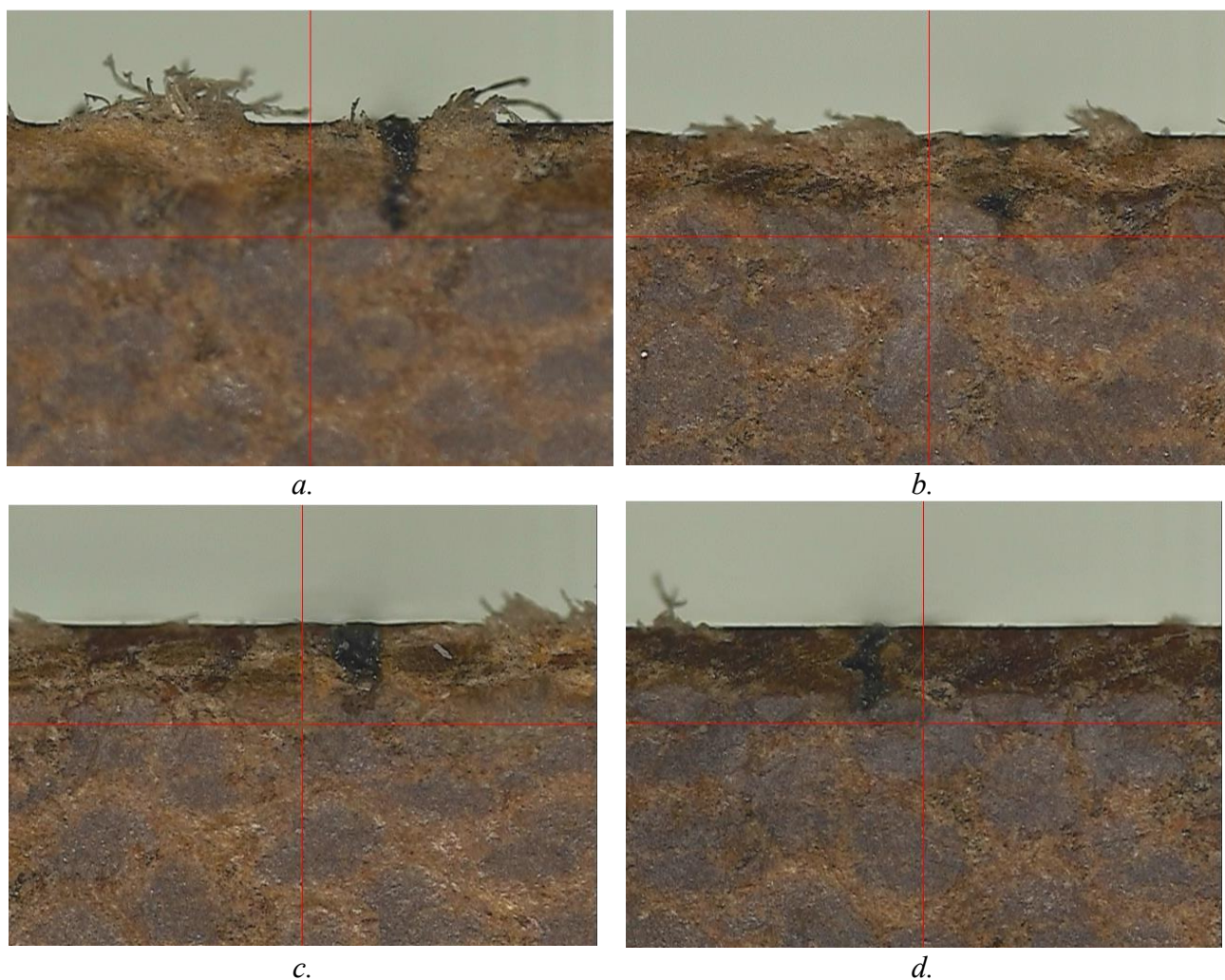


*Fig.4.19. Influence of the frequency of the laser pulse on the line profile when marking textolite samples with  $V_c=50$  mm/s and  $P = 30$  W,  $\times 30$ :*

*a –  $f=50$  kHz; b –  $f=60$  kHz; c –  $f=70$  kHz; d –  $f=80$  kHz*

#### **4.4. Conclusions**

1. Dependencies have been developed for changing the geometric parameters of the laser line (depth and width) depending on the marking speed ( $20 \div 250$  mm/s) and the output power ( $5 \div 50$  W).

2. It has been proven that during laser marking at a speed of  $50 \div 250$  mm/s on layered reinforced composites the depth of the marking line changes according to a linear law only at a radiation power of up to 20 W. At powers above 20W and marking speeds of  $50 \div 200$  mm/s, the depth changes according to a parabolic law, which is more pronounced at low marking speeds.

3. It has been proven that with an increase in the marking speed from 50 to 250 mm/s, for both studied materials, the depth of the marking lines decreases by about  $5 \div 7$  times, which is a result of the shorter time for thermal impact on the treated surfaces.

4. It has been proven that at a constant marking speed of 50 mm/s and an increase in the laser beam power from 5 to 50 W, the marking width for textolite samples increases from 180 to 1500  $\mu\text{m}$  –  $\approx 8$  times, and for glass textolite samples from 177 to 2080  $\mu\text{m}$  –  $\approx 12$  times.



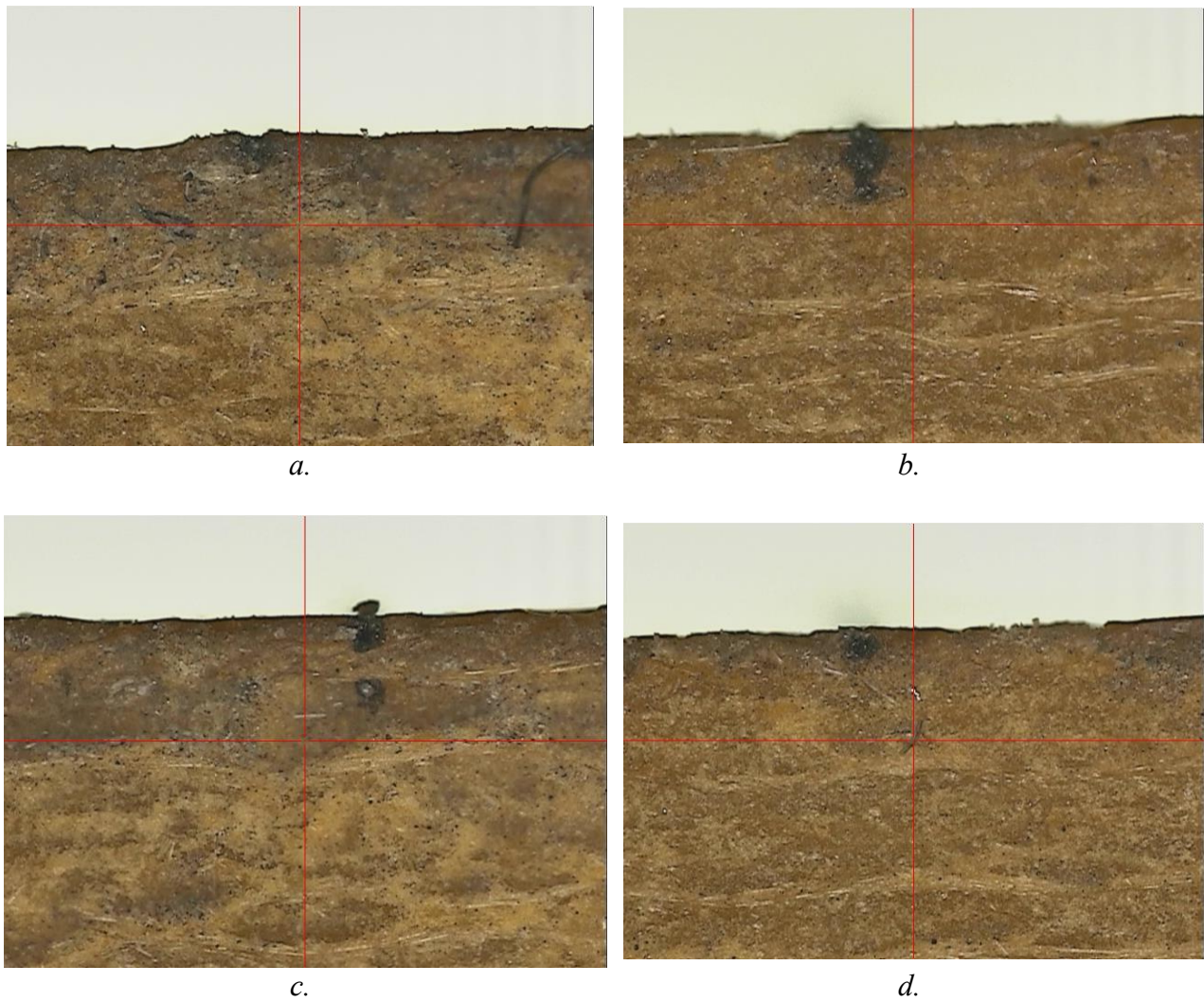


*Fig.4.20. Influence of the frequency of the laser pulse on the line profile when marking glass textolite samples with  $V_c=50$  mm/s and  $P = 15$  W,  $\times 30$ :*

*a –  $f=50$  kHz; b -  $f=60$  kHz; c -  $f=70$  kHz; d -  $f=80$  kHz*

5. It has been found that the higher values of the geometric parameters of the glass textolite samples compared to those of the textolite are the result of both the lower values of the roughness (which are commensurate with the wavelength of the laser beam), and the fact that the values of the Martens heat resistance and the specific heat of the textolite samples are  $160$  °C and  $0.446$  cal/g.°C, respectively, and are significantly higher compared to those of the glass textolite,  $105$ °C and  $0.20$  cal/g.°C, respectively.

6. It has been proven that with an increase in the power of the laser radiation from  $10$  to  $50$  W, the marking profile passes from a pseudo-planar to one resembling Gaussian distribution of the points of the contour. This is more pronounced in the textolite samples, because the textile reinforcing phase has a lower heat resistance compared to the glass one.

7. It has been shown that as frequency increases from  $50$  to  $80$  kHz, the profile of the marking channel changes from a Gaussian contour distribution to a pseudo-planar one. This is a result of the weaker penetration of the laser beam into the processed material at higher pulse frequency values.

## **Chapter Five: Composition of Mathematical Models and Optimization of Technological Processes**

From the material presented in the third and fourth chapters, it can be concluded that the mechanism of laser marking of layered reinforced composites with polymer matrix is a complex and

multifactorial process. In order to analyze the influence of technological factors on the geometry of the marking, it is necessary to compile mathematical models of the technological processes and conduct a dispersion analysis – ANOVA (Analysis of Variance).

The input factors and the factor space were selected on the basis of preliminary experiments and analysis of literature sources [1, 15, 49, 87]. For the studied technological process, a model was selected in which the output power of the beam –  $X_1$ , and the marking speed –  $X_2$ , were selected as input factors.

The objective functions are the geometric characteristics of the marking, which for glass textolite samples are penetration depth –  $Y_1$  and mark width –  $Y_2$ , and for textolite samples are penetration depth –  $Y_3$  and mark width –  $Y_4$ .

The studies were conducted at constant values of:

- the frequency of the laser pulse –  $f = 50$  kHz
- raster inclination –  $\alpha = 0^\circ$
- defocus –  $S = 0$  mm
- marking repeatability –  $R = 1$

the studied samples were irradiated by the laser beam directly under normal conditions and the following beam characteristics:

- wavelength –  $\lambda = 1064$  nm
- focal spot diameter –  $d_f = 40$   $\mu$ m

The main values of the input factors, as well as the variation intervals when marking the samples are presented in Table 5.1.

Based on the accumulated experimental results in Tables 4.1÷4.4, the experimental plan was completed – Table 5.2.

*Table 5.1. Areas of factor variation*

factor levels	$X_1, W$	$X_2, \text{mm/s}$	coded value
$X_{i0} + \Delta X_i$	45	250	+1
$X_{i0}$	25	150	0
$X_{i0} - \Delta X_i$	5	50	-1

*Table 5.2. Experiment plan*

Nº	$X_0$	$X_1$	$X_2$	$X_1 X_2$	$X_1^2$	$X_2^2$	$Y_1$	$Y_2$	$Y_3$	$Y_4$
1	+1	+1	+1	+1	+1	+1	281	1193	182	748
2	+1	-1	+1	-1	+1	+1	31	377	18	0
3	+1	+1	-1	-1	+1	+1	1440	1893	818	1358
4	+1	-1	-1	+1	+1	+1	160	377	91	183
5	+1	+1	0	0	+1	0	469	1627	273	1128
6	+1	-1	0	0	+1	0	52	153	30	92
7	+1	0	+1	0	0	+1	156	416	91	323
8	+1	0	-1	0	0	+1	800	1136	455	770
9	+1	0	0	0	0	0	260	889	152	615

### **5.1. Mathematical models of technological parameters when marking glass textolite parts**

The obtained regression model for determining the penetration depth of laser radiation in glass textolite –  $Y_1$  takes the form 5.2, and the graphical interpretation of the results in two and three coordinate systems is presented in Fig. 5.1.

$$Y_1 = 405.444 + 324.500x_1 - 322.000x_2 - 257.500x_1x_2 \quad (5.2)$$

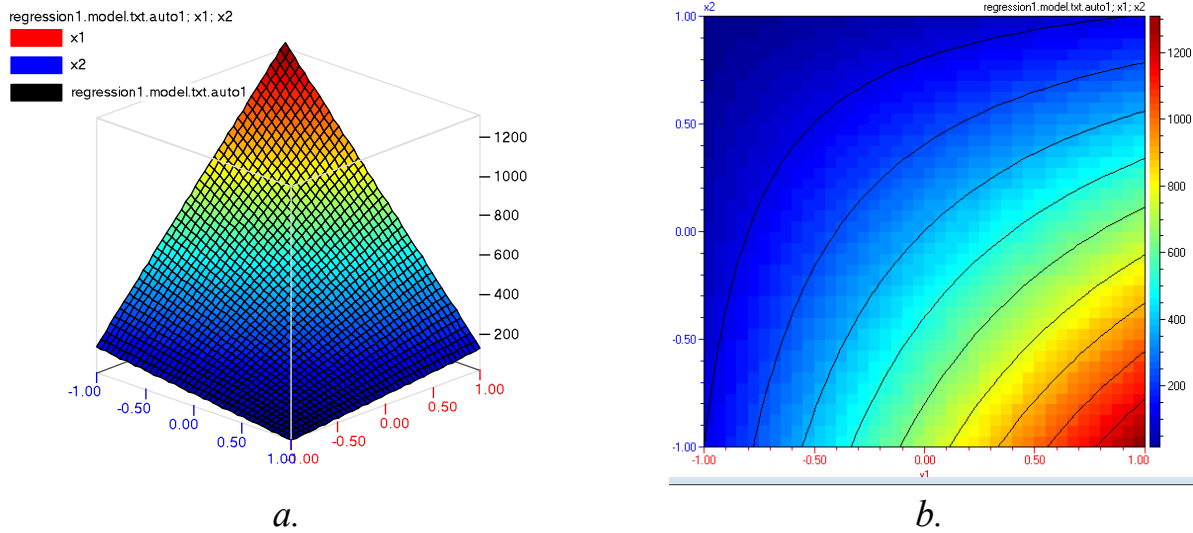


Fig.5.1. Graphical representation of the dependence  $Y_1 = f(X_1, X_2)$   
*a – in three-coordinate system; b – in two-coordinate system*

The obtained regression model for determining the width of the marking stroke in glass textolite samples (5.4) has a graphical interpretation shown in Fig. 5.4.

$$Y_2 = 895.667 + 634.333x_1 - 236.667x_2 \quad (5.4)$$

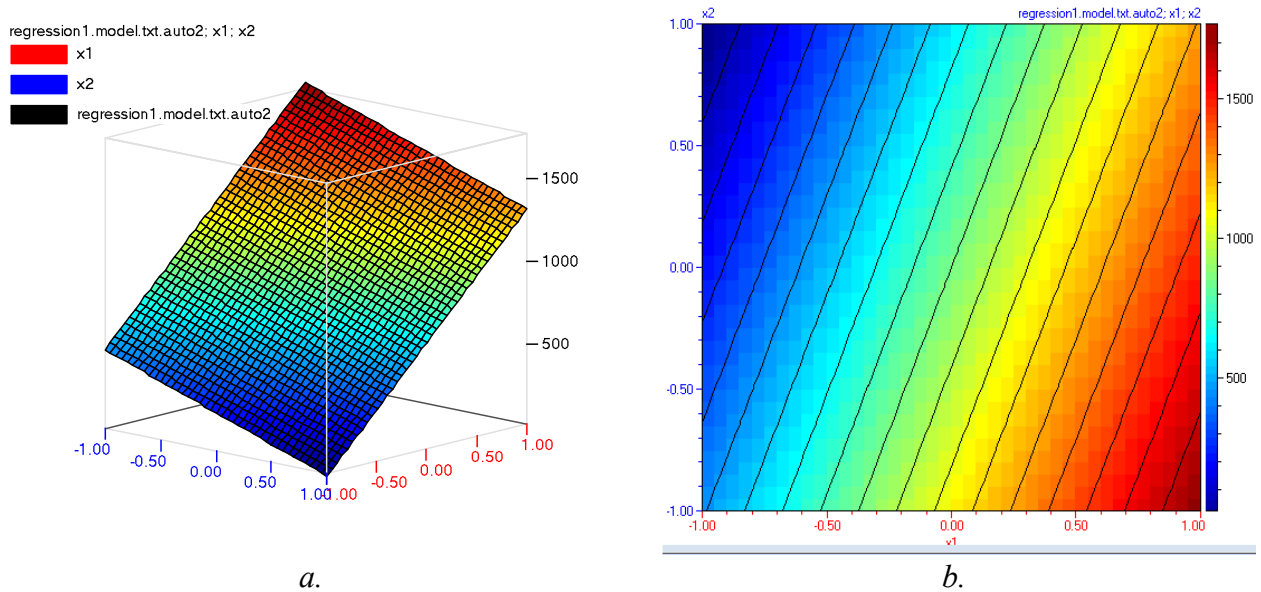


Fig.5.4. Graphical representation of the dependence  $Y_2 = f(X_1, X_2)$   
*a – in three-coordinate system; b – in two-coordinate system*

## 5.2. Mathematical models of technological parameters when marking textolite parts

The obtained regression model for determining the depth of penetration of laser radiation into textolite –  $Y_3$  takes the form 5.6, and the graphical interpretation of the results in two and three coordinate systems is presented in Fig.5.7.

$$Y_3 = 232.667 + 189.000x_1 - 178.833x_2 - 140.750x_1x_2 + 2.667x_1x_1 \quad (5.6)$$

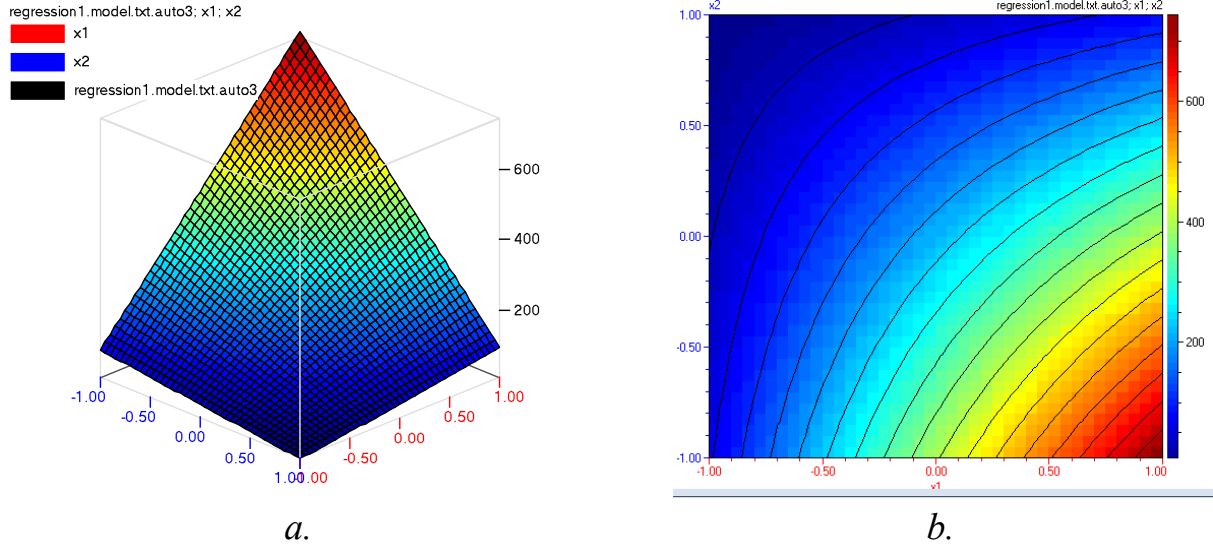


Fig.5.7. Graphical representation of the dependence  $Y_3 = f(X_1, X_2)$   
a – in three-coordinate system; b – in two-coordinate system

The obtained regression model for determining the width of the marking stroke on textolite samples (5.8) has a graphical interpretation shown in Fig. 5.10.

$$Y_4 = 569.333 + 493.167x_1 - 206.667x_2 - 106.750x_1x_2 + 15.500x_1^2 \quad (5.8)$$

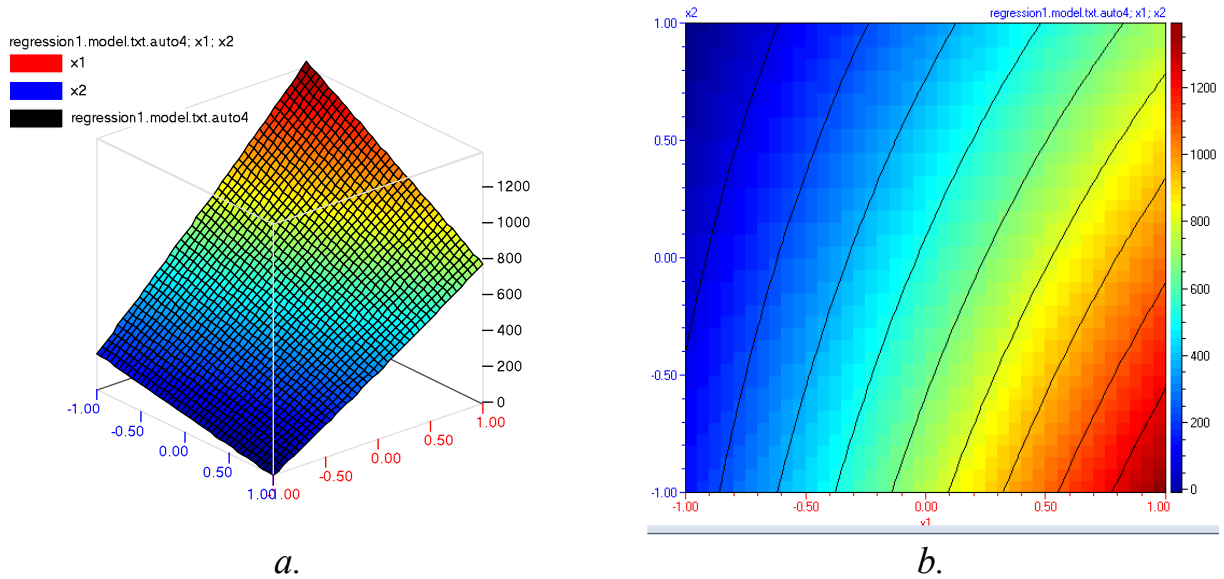


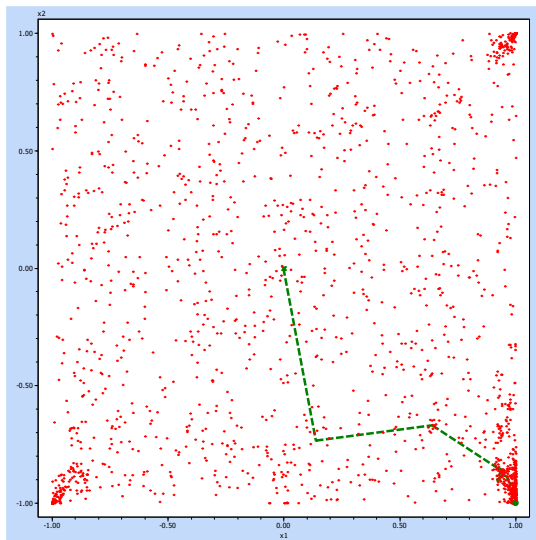
Fig.5.10. Graphical interpretation of the dependence  $Y_4 = f(X_1, X_2)$   
a – in three-coordinate system; b – in two-coordinate system

### 5.3. Optimization of technological parameters

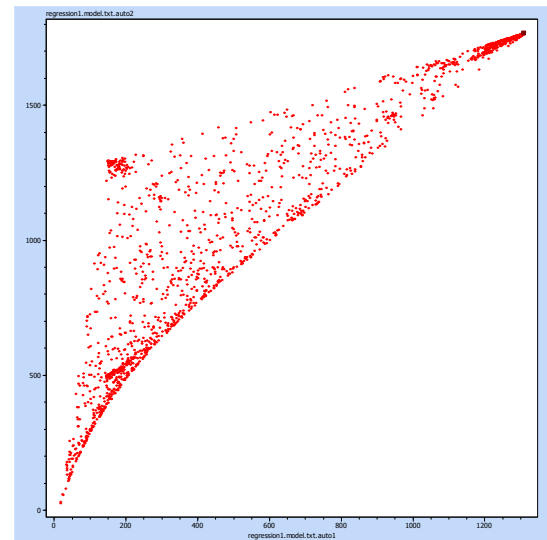
#### 5.3.1. Optimization of the process of marking glass textolite materials

The optimization of the technological process for marking glass textolite samples was made based on the given values  $Y_{1max}$  and  $Y_{2max}$ .

The optimization was made using a non-dominated sorted genetic algorithm II (NSGA II) and is presented as a result in Appendix No 1.5, and the graphical interpretation is shown in Fig. 5.13.



a.



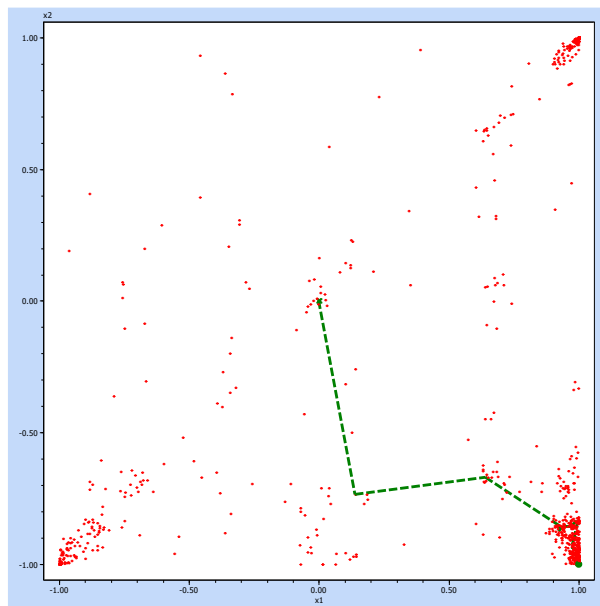
b.

Fig.5.13. Pareto front of the maximum of  $Y_1$  and  $Y_2$

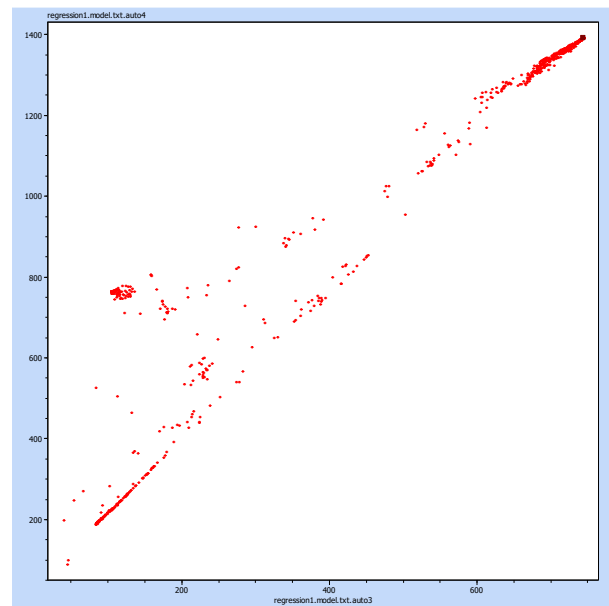
### 5.3.2. Optimization of the process of marking textolite materials

The optimization of the technological process for marking textolite samples was made based on the given values  $Y_3\max$  and  $Y_4\max$ .

The optimization was made using a non-dominated sorted genetic algorithm II (NSGA II) and is presented as a result in Appendix No. 1.6, and the graphical interpretation is shown in Fig. 5.14.



a.



b.

Fig.5.14. Pareto front of the maximum of  $Y_3$  and  $Y_4$

## CONTRIBUTIONS OF THE DISSEERTATION

The results obtained in the research process allow for the formulation of contributions in two main areas – scientific-applied (original and confirmatory) and applied.

### A. Scientific-applied contributions

#### *A.1. Creation of new classifications, methods, designs, models, methodologies*

□ Conceptual model for the development of a laser installation for marking layer-reinforced composites on a polymer basis.

□ Mathematical models of the influence of beam power and marking speed on the penetration depth and width of the laser stroke in laser marking of textolite and glass textolite.

#### ***A.2. Obtaining and proving new facts***

□ The responses of two materials (textolite and glass textolite) in terms of the characteristics of the marking stroke, caused by the parameters of the laser marking process, have been established.

#### **B. Applied contributions**

□ A workable laser system for marking layer-reinforced polymer-based composites.

### **DOCTORAL PUBLICATIONS**

1. **Tsenkulovski, S.**, I. Mitev, G. Karlovski, Factors Influencing the Laser Marking of Non-metal Materials, XXXII International Scientific Symposium “Metrology and Metrology Assurance 2022”, Sozopol, 2022, pp. 54÷58. ISSN 978-1-6654-8569-2/22

2. **Tsenkulovski, S.**, I. Mitev, G. Karlovski, Determination of the Penetration Depth of Lazer Marking of Polimeric Materials, XXXII International Scientific Symposium “Metrology and Metrology Assurance 2022”, Sozopol, 2022, pp. 59÷62. ISSN 978-1-6654-8569-2/22.

3. Mitev, I., **S. Tsenkulovski**, G. Karlovski, Determination of the Penetration Depth of Laser Marking of Glass Fiber Reinforced Polymers, XXXIII International Scientific Symposium “Metrology and Metrology Assurance 2023”, Sozopol, 2022, pp.34÷38, ISSN 2603-3194.

4. Mitev, I., **S. Tsenkulovski**, Local Processing of Non-Metal Materials with Concentrated Energy Flow, 14<sup>th</sup> ISPC “Environment Technology Resources”, Rezekne, Latvia, Vol. 3, 15÷16 June, 2023, pp.183÷186, ISSN 1691-5402 print; ISSN 2256-070X online Scopus

5. **Tsenkulovski, S.**, Mitev, I., Elements of the energy balance in laser marking of layered reinforced composites with a polymer matrix, “Industrial Technologies”, vol. 1., p.11, 2024, c.198÷203, ISSN 1314-9911.

6. Mitev, I., **Tsenkulovski, S.**, Influence of the Technological Parameters of the Laser Marking Process on the Strike Width in Layer Reinforced Composites with a Polymer Matrix, “Industrial technologies”, vol. 11 (1), 2024, p.204÷208, ISSN 1314-9911.

7. **Tsenkulovski, S.**, I. Mitev, Influence of the Parameters of the Lasser marking process of the depth of penetration in layer-reinforced composites, 15<sup>th</sup> ISPC “Environment Technology Resources”, vol. 3, V.Turnovo, Bulgaria, 27 and 28 06.2024, p. 319÷324, ISSN 1691-5402 print; ISSN 2256-070X online Scopus

8. **Tsenkulovski, S.**, Penetration Depth in Laser Marking of Composite Materials with Textile Reinforcement Phase, Journal of Technical University of Gabrovo, vol.70, 2025, ID JTUG-2025-0002



# **TITLE: PECULIARITIES OF LASER MARKING OF LAYER-REINFORCED COMPOSITES ON A POLYMER BASIS**

**Author: mag. eng. Simeon Tsankov Tsenkulovski**

**ABSTRACT:** *The lack of systematic information on the laser marking of layered reinforced polymer-based composite materials limits the application of this method in industry. For reliable prediction and optimization of the technological process of laser marking of these materials, it is necessary to scientifically investigate it.*

*In this study, based on an in-depth study, a conceptual model of a system for laser marking of layered reinforced composites with a polymer matrix (textolite and glass-textolite) has been formed. Based on the model, a system with a Fiber laser – RFL- P - 502B with an optical lens F-theta lens–SL – 1064-150-2106 has been manufactured.*

*The interaction of the laser beam with the substance during local processing of non-metallic materials has been examined. The stages of the laser marking process of non-metallic materials have been traced and an energy balance equation has been derived.*

*Experiments were conducted to determine the influence of the technological parameters of the laser marking process (radiation power and marking speed) on the geometric characteristics of the laser stroke (depth, width and cross-section of the channel) and graphical dependencies were drawn up for the relationship between them.*

*Based on regression analysis, mathematical models describing the influence of the technological parameters of the process on the geometry of the laser stroke have been compiled and optimization of the process has been performed using the non-dominated sorted genetic algorithm II (NSGA II).*

**Keywords:** *laser marking, layered reinforced composites with polymer matrix, geometric parameters of the laser stroke, mathematical models, optimization*